nature neuroscience

Spinal cord injury-induced immunodeficiency is mediated by a sympathetic-neuroendocrine adrenal reflex

Harald Prüss[1–3], Andrea Tedeschi[4–6], Aude Thiriot[1], Lydia Lynch[1], Scott M Loughhead[1], Susanne Stutte[1,7], Irina B Mazo[1], Marcel A Kopp[2], Benedikt Brommer[2,4], Christian Blex[2], Laura-Christin Geurtz[2], Thomas Liebscher[8], Andreas Niedeggen[8], Ulrich Dirnagl[2,3], Frank Bradke[5], Magdalena S Volz[9], Michael J DeVivo[10], Yuying Chen[10], Ulrich H von Andrian[1,12] & Jan M Schwab[2,11,12]

Acute spinal cord injury (SCI) causes systemic immunosuppression and life-threatening infections, thought to result from noradrenergic overactivation and excess glucocorticoid release via hypothalamus–pituitary–adrenal axis stimulation. Instead of consecutive hypothalamus–pituitary–adrenal axis activation, we report that acute SCI in mice induced suppression of serum norepinephrine and concomitant increase in cortisol, despite suppressed adrenocorticotropic hormone, indicating primary (adrenal) hypercortisolism. This neurogenic effect was more pronounced after high-thoracic level (Th1) SCI disconnecting adrenal gland innervation, compared with low-thoracic level (Th9) SCI. Prophylactic adrenalectomy completely prevented SCI-induced glucocorticoid excess and lymphocyte depletion but did not prevent pneumonia. When adrenalectomized mice were transplanted with denervated adrenal glands to restore physiologic glucocorticoid levels, the animals were completely protected from pneumonia. These findings identify a maladaptive sympathetic-neuroendocrine adrenal reflex mediating immunosuppression after SCI, implying that therapeutic normalization of the glucocorticoid and catecholamine imbalance in SCI patients could be a strategy to prevent detrimental infections.

The CNS modulates immune system function[1–3]. SCI causes acute secondary immunosuppression, referred to as SCI-induced immune deficiency syndrome (SCI-IDS)[4–8]. The neurogenic origin of SCI-IDS renders patients with SCI lesions highly susceptible to infections[9], with pneumonia being the leading cause of early death (32%), even after correcting for other risk factors such as immobility, aspiration or ventilation[10]. Pneumonia occurs in up to 45% of SCI patients[11] and represents an independent risk factor for poor neurological and functional long-term outcome associated with reduced intrinsic recovery potential[12,13].

The mechanisms by which the CNS induces immunosuppression are signaled through the immune system–nervous system interfaces: (i) the hypothalamus–pituitary–adrenal (HPA) axis regulating glucocorticoid (GC) release from the adrenal glands, (ii) the sympathetic nervous system innervating abdominal organs and the catecholamine (CA)-releasing areas of the adrenals and (iii) the parasympathetic nervous system, i.e., the vagus nerve, which bidirectionally connects the brainstem with most visceral organs[14–16]. Recent reports delineated the role of secondary immune organs centering on the spleen[9,17]. Despite responding to SCI with remarkable atrophy, blocked sympathetic signaling to the spleen was not able to reduce infection susceptibility to baseline levels after SCI, suggesting the existence of additional neurogenic pathomechanisms[9]. We set out to investigate the role of sympathetic denervation of the adrenal gland after SCI as a candidate pathway to elicit systemic changes. Classical concepts posit that SCI-induced immunosuppression is mainly mediated by stress-related noradrenergic overactivation and excess GC release via the HPA axis. Given that immunosuppression is differentially modulated by lesion localization, a critical role for central and peripheral neuronal circuits, as well as for immune organ innervation, has been suggested[18,19].

However, it is unknown (i) whether changes in systemic GC and CA levels in the acute phase after SCI and the injury-induced immunosuppression result from direct denervation of immune organs[20,21] or from humoral mechanisms (i.e., circulating mediators) and (ii) whether fluctuations of lymphocytes are epiphenomena or cause clinically relevant infections. Insights into these mechanisms are of exceptional clinical importance because of the profoundly increased rate of infectious complications in SCI patients[11]. For this, we first analyzed the kinetics and sources of CAs and GCs after experimental

[1]Department of Microbiology and Immunobiology, Division of Immunology, Harvard Medical School, Boston, Massachusetts, USA. [2]Department of Neurology and Experimental Neurology, Clinical and Experimental Spinal Cord Injury Research (Neuroparaplegiology), Charité – Universitätsmedizin Berlin, corporate member of Freie Universität Berlin, Humboldt-Universität zu Berlin, and Berlin Institute of Health, Berlin, Germany. [3]German Center for Neurodegenerative Diseases (DZNE), Berlin, Germany. [4]Boston Children's Hospital, F.M. Kirby Neurobiology Center, Center for Life Science, Harvard Medical School, Boston, Massachusetts, USA. [5]German Center for Neurodegenerative Diseases (DZNE), Bonn, Germany. [6]Center for Brain and Spinal Cord Repair, Department of Neuroscience, The Neurological Institute, The Ohio State University Wexner Medical Center, Columbus, Ohio, USA. [7]Institute for Immunology, Biomedical Center, Ludwig-Maximilians-University Munich, Martinsried, Germany. [8]Treatment Centre for Spinal Cord Injuries, Trauma Hospital Berlin, Berlin, Germany. [9]Department of Gastroenterology, Infectiology and Rheumatology, Charité – Universitätsmedizin Berlin, Berlin, Germany. [10]National Spinal Cord Injury Statistical Center, Department of Physical Medicine and Rehabilitation, University of Alabama at Birmingham, Birmingham, Alabama, USA. [11]Department of Neurology and Neuroscience, Center for Brain and Spinal Cord Repair, Department of Physical Medicine and Rehabilitation, The Neurological Institute, The Ohio State University Wexner Medical Center, Columbus, Ohio, USA. [12]These authors contributed equally to this work. Correspondence should be addressed to U.H.v.A. (uva@hms.harvard.edu).

Received 5 April; accepted 24 August; published online 18 September 2017; doi:10.1038/nn.4643

SCI in mice and compared the data with that from human SCI patients to specifically investigate effects of the sympathetic nervous system. By applying complete transections at different anatomical sites in the SCI model, we evaluated the role of neurogenic level-dependent innervation to immune and endocrine organs for cellular changes and susceptibility to infection. In contrast to the classically considered disease model of SCI-induced immunosuppression caused by HPA axis activation or topical denervation of lymphoid organs, our results delineate an alternative pathway for a lesion-level-dependent maladaptive neuroendocrine response.

RESULTS

Lesion-level-dependent SCI effects on systemic norepinephrine and GC levels

We first determined the kinetics of norepinephrine (NE) and GC levels after experimental injury. For this, SCI was induced in mice at Th1 or Th9 with a microknife following the experimental design indicated in **Figure 1a**; sham controls received laminectomy only. Lesion-level-dependent injury of sympathetic preganglionic neurons localized to the intermediolateral columns and funiculus lateralis in the thoracic rodent spinal cord was assured by a complete spinal cord transection. Based on current CNS injury models, we expected NE ('adrenergic storm') and GC to increase, partly due to stress-induced adrenocorticotropic hormone (ACTH) release (which stimulates corticosterone) and sympathetic nervous system activation (i.e., NE release from the adrenal medulla). Instead, systemic NE levels were profoundly suppressed after experimental high-level SCI while NE levels after low-level SCI were not affected (**Fig. 1b**), likely reflecting the loss of adrenal innervation after complete Th1 versus Th9 transection. As expected, serum corticosterone levels were markedly increased after Th1 SCI (**Fig. 1c**). However, the increase was not a result of stress-related HPA axis stimulation from pituitary ACTH release, as ACTH was suppressed after high-level SCI (**Fig. 1d**). Instead, GC release represents primary hypercortisolism following adrenal gland denervation (disinhibition), similarly to a steroid-producing adrenal tumor. In line with this finding

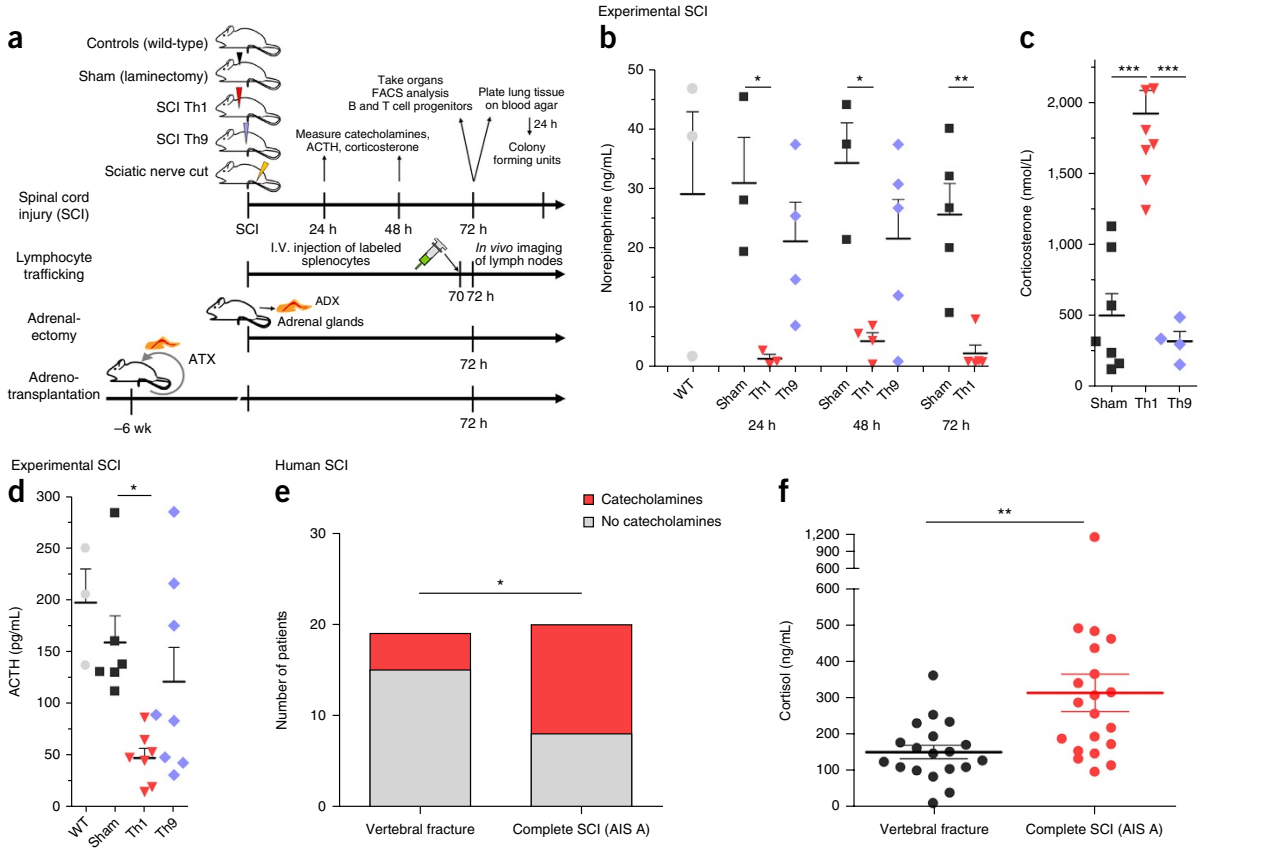

Figure 1 SCI-IDS is lesion-height-dependent and associated with major changes in CA and GC levels in both murine experimental SCI and human SCI. (**a**) Schematic showing the timeline of the experimental SCI protocol and subsequent analyses. (**b**) SCI above the level of the adrenal gland innervation (Th1), but not below (Th9), resulted in a profound drop in plasma norepinephrine levels between 1 and 3 d after experimental SCI (one-way ANOVA, $P = 0.0375$, $F = 5.445$, $df = 9$ (24 h); $P = 0.0211$, $F = 6.105$, $df = 11$ (48 h); with Tukey's multiple comparison test, $^{*}P < 0.05$; unpaired Student's t test, $^{**}P = 0.027$, $t = 4.266$, $df = 8$ (72 h); data are mean ± s.e.m., $n = 3$ animals in each group (sham-operated (sham) 24 h, Th1-lesioned (Th1) 24 h, sham 48 h), 4 animals in each group (Th9-lesioned (Th9) 24 h, Th1 48 h) or 5 animals in each group (Th9 48 h, sham 72 h, Th1 72 h)). (**c**) Th1 SCI, but not Th9 SCI, resulted in a profound increase in serum corticosterone 3 d after SCI (one-way ANOVA, $P < 0.0001$, $F = 31.62$, $df = 19$, with Tukey's multiple comparison test, $^{***}P < 0.001$; data are mean ± s.e.m., $n = 7$ animals in each group (sham, Th1) or 4 animals (Th9)). (**d**) However, ACTH levels were suppressed, which reflects primary hypercortisolism and not HPA-axis stimulation (one-way ANOVA, $P = 0.0249$, $F = 4.563$, $df = 20$, with Tukey's multiple comparison test, $^{*}P < 0.05$; data are mean ± s.e.m., $n = 6$ animals (sham), 7 animals (Th1), 8 animals (Th9)). (**e**) Patients with complete SCI (American Spinal Injury Association impairment scale (AIS) grade A) frequently required CAs within the first 96 h after SCI, whereas control patients undergoing spinal surgery for vertebral fracture did not (Fisher's exact test, $^{*}P = 0.023$; data are absolute frequencies, $n = 19$ controls, 20 complete SCI patients). (**f**) In human SCI patients, cortisol levels were similarly increased over controls within the first 96 h after injury (unpaired Student's t test, $^{**}P = 0.0062$, $t = 2.902$, $df = 37$; data are mean ± s.e.m., $n = 19$ controls, 20 complete SCI patients).

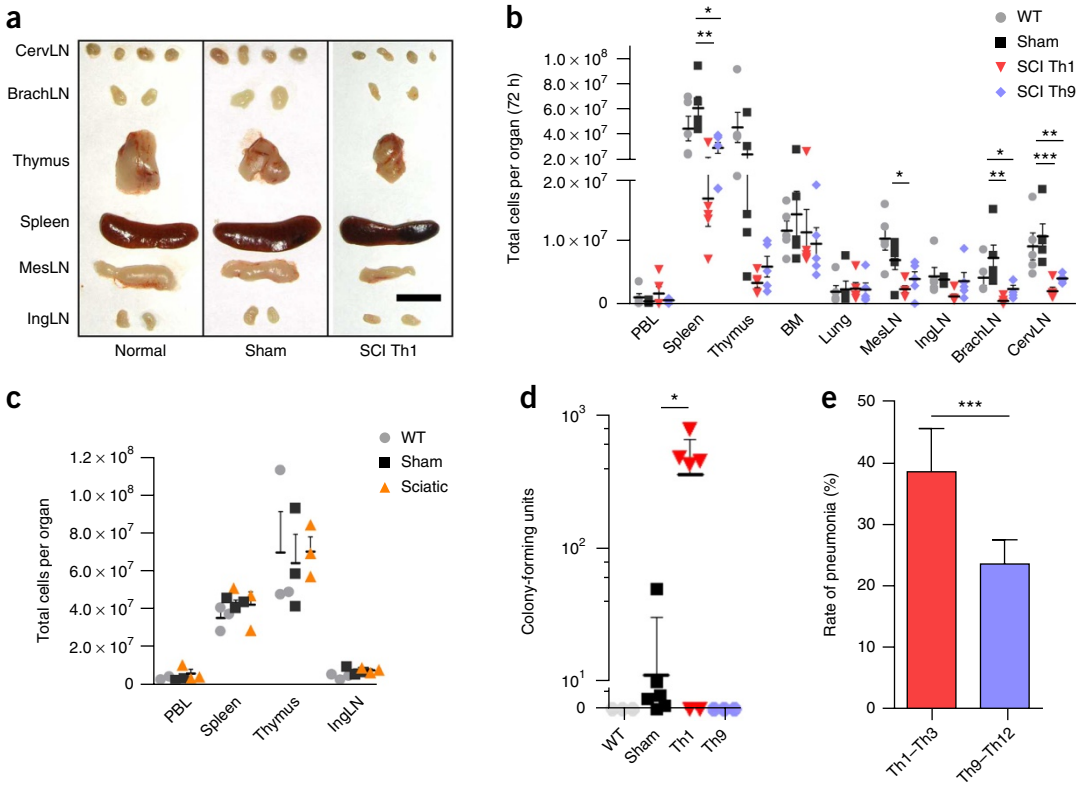

Figure 2 SCI resulted in lymphoid organ involution, leukocyte depletion and spontaneous pneumonia. (**a**) SCI, but not sham surgery, led to profound shrinkage after 72 h in (from top) cervical lymph nodes (cervLN), brachial LN (brachLN), thymus, spleen, mesenteric LN (mesLN) and inguinal LN (ingLN). Scale bar, 5 mm. (**b**) Cell loss was related to the level of SCI. Organ reduction after 72 h was more pronounced if the lesion was above innervation of abdominal organs (Th1 vs. Th9), with the exception of BM (one-way ANOVA, $P = 0.3375$, $F = 1.191$, $df = 14$ (peripheral blood leukocytes, PBL); $P = 0.0012$, $F = 12.49$, $df = 14$ (spleen); $P = 0.0515$, $F = 3.835$, $df = 14$ (thymus); $P = 0.6186$, $F = 0.5001$, $df = 14$ (BM); $P = 0.9949$, $F = 0.0051$, $df = 14$ (lung); $P = 0.0425$, $F = 4.158$, $df = 14$ (mesLN); $P = 0.0748$, $F = 3.244$, $df = 14$ (ingLN); $P = 0.0056$, $F = 8.221$, $df = 14$ (brachLN); $P = 0.0007$, $F = 14.19$, $df = 14$ (cervLN); with Tukey's multiple comparison test, $^*P < 0.05$; $^{**}P < 0.01$; $^{***}P < 0.001$; data are mean ± s.e.m., $n = 5$ animals per group). (**c**) Further distal, postganglionary lesioning of the nervous system (sciatic nerve dissection) had no effect on organ cellularity (unpaired Student's t test, $P = 0.3626$, $t = 1.071$, $df = 3$ (PBL); $P = 0.9040$, $t = 0.1284$, $df = 4$ (spleen); $P = 0.7409$, $t = 0.3545$, $df = 4$ (thymus); $P = 0.6888$, $t = 0.4308$, $df = 4$ (ingLN); data are mean ± s.e.m., $n = 3$ animals per group). (**d**) High-lesion animals (Th1) were much more susceptible to spontaneous pneumonia than nonoperated, sham-operated or Th9-lesioned mice (one-way ANOVA, $P = 0.0184$, $F = 5.679$, $df = 14$; with Tukey's multiple comparison test, $^*P < 0.05$; data are mean ± s.e.m., $n = 3$ animals (Th9), 6 animals per group (sham, Th1)). (**e**) Similarly, after SCI in humans, patients with high thoracic lesions (Th1–Th3, $n = 182$ patients from the National Spinal Cord Injury Database) showed enhanced susceptibility to pneumonia during acute care or inpatient rehabilitation compared to those with low thoracic lesions (χ^2 test, $^{***}P < 0.001$; data are relative frequencies ± 95% CI, $n = 461$ (Th9–Th12), 182 (Th1–Th3)).

suggesting an innervation-dependent effect, we observed no GC increase after a low-level SCI (Th9) in which most fibers innervating the adrenal glands were spared (**Fig. 1c**).

Similar changes in NE and GC levels were also seen after human traumatic SCI. Patients with complete SCI, which is associated in over 93% of cases with a complete sympathetic lesion[22], frequently required CA treatment in clinical routine during the first days after injury to compensate for symptoms of CA deficiency, such as hypotension or bradycardia (**Fig. 1e**). By contrast, no such CA requirement was detected in control patients undergoing spinal surgery only (**Fig. 1e**). Cortisol levels were significantly increased in SCI patients over controls within the first 96 h (median 19 h, interquartile range 4.25–33.5 h) after the injury (**Fig. 1f**). Significant differences were still seen after adjustment for age, sex and multiple injuries within a linear regression model (coefficient = 0.332; 95% confidence interval (CI) 0.122–0.543; $P = 0.003$, adjusted $R^2 = 0.179$). None of the patients received cortisol treatment after SCI. In sum, early endocrine changes after SCI are characterized by systemic CA depletion and GC increase, thus pointing to SCI-induced abnormal functions of the adrenal glands, which produce the majority of circulating NE and GC.

SCI induces severe leukopenia and spontaneous pneumonia

We next examined how SCI-induced endocrine changes are paralleled by depletion of leukocytes (a hallmark of SCI-IDS) and susceptibility to lung infection. SCI resulted in marked atrophy of lymphoid tissue (**Fig. 2a**) and a massive loss of total cell numbers in most immune organs after 3 d (**Fig. 2b**). The effects depended on the level of SCI, with the largest cell reduction after high-level (Th1) compared to low-level (Th9) injury (**Fig. 2b**). These changes started early and were detectable already at 1 and 2 d after SCI (**Supplementary Fig. 1**). The profound cell loss affected all major immune cell populations and changed lymph node (LN) morphology, including $CD19^+$ B cells, $CD4^+$ and $CD8^+$ T cells, $CD11c^+$ dendritic cells (DCs), $CD11b^+$ monocytes, and $NK1.1^+$ NK cells (**Supplementary Fig. 2**). Further distal (postganglionary) lesioning of the nervous system, i.e., sciatic nerve dissection versus sham surgery, had no effect on systemic changes of thymus and spleen

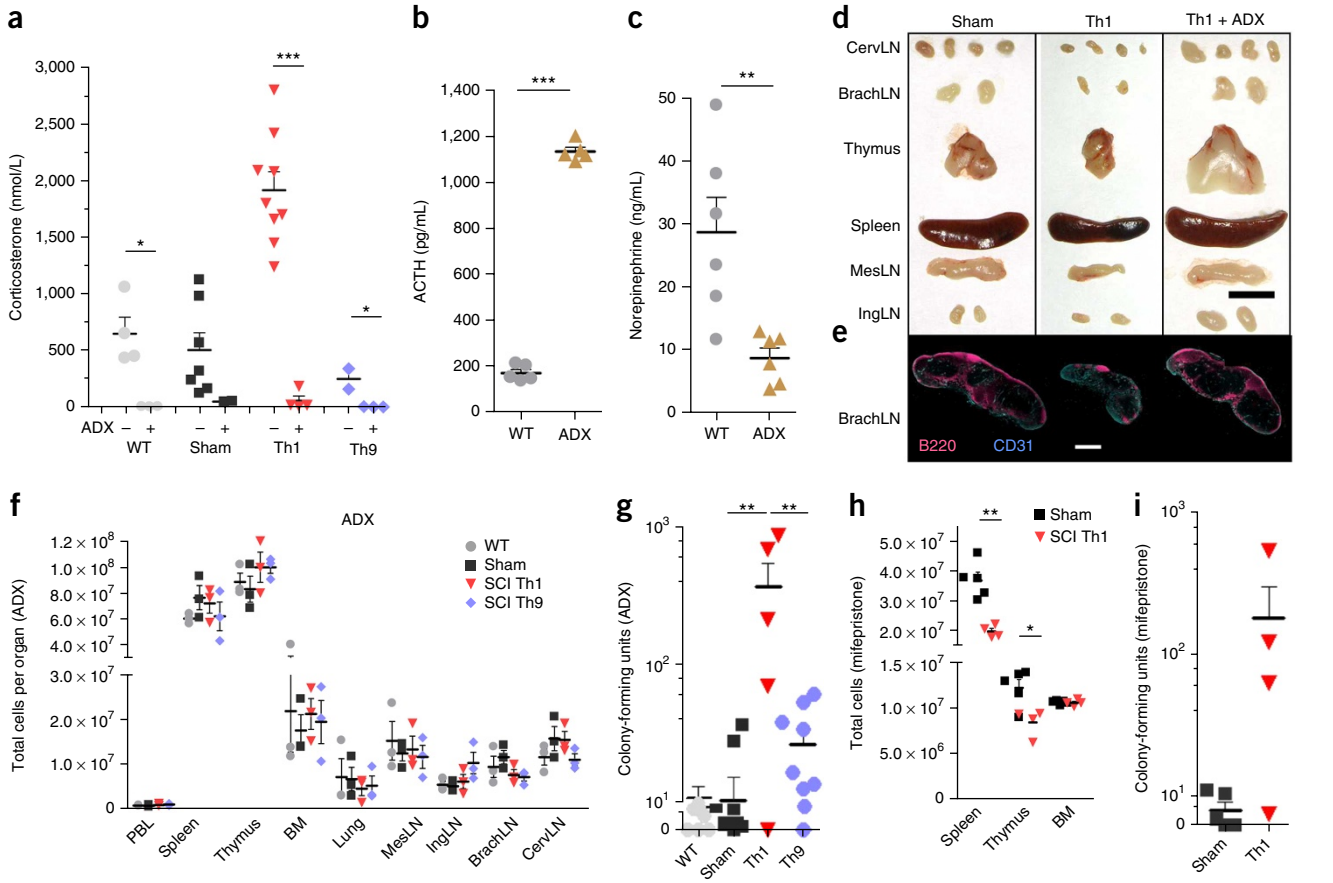

Figure 3 Interventional effects of ADX after acute SCI. (**a**) Serum corticosterone levels were completely depleted in all surgery conditions after ADX 3 d after SCI (unpaired Student's *t* test, $*P = 0.0136$, $t = 3.730$, $df = 5$ (wild-type mice; WT); $*P = 0.1745$, $t = 1.511$, $df = 7$ (sham); $***P < 0.0001$, $t = 7.413$, $df = 11$ (Th1); $*P = 0.0349$, $t = 3.676$, $df = 3$ (Th9); data are mean ± s.e.m., $n = 3$ animals in each group (WT + ADX, sham + ADX, Th9), 4 animals in each group (WT + no ADX, Th1+ADX), 7 animals (sham + no ADX), 9 animals (Th1 + no ADX)). (**b**) ACTH levels responded physiologically with increased secretion (unpaired Student's *t* test, $***P < 0.0001$, $t = 39.69$, $df = 8$; data are mean ± s.e.m., $n = 5$ animals per group). (**c**) ADX further resulted in ~60–70% reduction in systemic NE (unpaired Student's *t* test, $**P = 0.0062$, $t = 3.455$, $df = 10$; data are mean ± s.e.m., $n = 6$ animals per group). (**d**–**f**) Bilateral ADX rescues quantitative immune depletion by completely reversing the massive organ shrinkage after SCI (**d**), preserving the LN architecture with B220$^+$ B cell follicles demonstrated for the brachial LN (**e**; red) and restoring cell numbers regardless of the level of SCI (**f**; one-way ANOVA, $P = 0.4030$, $F = 1.061$, $df = 8$, (PBL); $P = 0.5700$, $F = 0.6183$, $df = 8$ (spleen); $P = 0.3709$, $F = 1.175$, $df = 8$ (thymus); $P = 0.8068$, $F = 0.2226$, $df = 8$ (BM); $P = 0.7822$, $F = 0.2560$, $df = 8$ (lung); $P = 0.8967$, $F = 0.1110$, $df = 8$ (mesLN); $P = 0.1551$, $F = 2.584$, $df = 8$, (ingLN); $P = 0.0796$, $F = 3.975$, $df = 8$ (brachLN); $P = 0.2639$, $F = 1.677$, $df = 8$ (cervLN); data are mean ± s.e.m., $n = 3$ animals per group). Scale bar in **d**, 5 mm; in **e**, 1 mm. (**g**) ADX, however, failed to reestablish functional immune defense after SCI, with high frequency of pneumonia in SCI animals with predominant susceptibility after high (Th1) lesions (one-way ANOVA, $P = 0.0043$, $F = 7.363$, $df = 21$, with Tukey's multiple comparison test, $**P < 0.01$; data are mean ± s.e.m., $n = 9$ animals (Th9), 8 animals (sham), 5 animals (Th1)). (**h**,**i**) Antagonism at the GC receptor, using mifepristone, partially prevented cell depletion, particularly in the thymus (**h**; unpaired Student's *t* test, $**P = 0.0010$, $t = 5.374$, $df = 7$ (spleen); $*P = 0.0171$, $t = 3.107$, $df = 7$ (thymus); $P = 0.8706$, $t = 0.1689$, $df = 7$ (BM); data are mean ± s.e.m., $n = 5$ sham and 4 Th1 animals), but it did not prevent lung infections (**i**; unpaired Student's *t* test, $P = 0.1400$, $t = 1.664$, $df = 7$; data are mean ± s.e.m., $n = 5$ sham and 4 Th1 animals).

cellularity (**Fig. 2c**). Th1-lesioned animals were highly susceptible to spontaneous pneumonia after 3 d, as documented by bacterial cultures of lung homogenates (**Fig. 2d**). By contrast, almost no bacteria were found in lungs of naive (wild-type), sham-operated or Th9-injured animals (**Fig. 2d**). In analogy, significantly elevated pneumonia rates were observed in patients with motor-complete high thoracic lesions (Th1–Th3) compared with low thoracic SCI (Th9–Th12; $n = 70$ of 182, 38.5% (95% CI 31.4–45.6%) versus $n = 109$ of 461, 23.6% (95% CI 19.7–27.5%), $P < 0.0001$; **Fig. 2e**).

Notably, although major cell loss in secondary lymphoid organs depended on the SCI level, LNs above high-level lesions (Th1) were similarly affected (**Fig. 2b**). Thus organ atrophy could not be explained by direct neural innervation to LNs (for example, cervical LN depletion) but must rather be mediated predominantly by circulating factors. This is further supported by our finding that sciatic nerve dissection was not associated with lymphocyte counts in the directly innervated structures. Specifically, peripheral nerve injury did not result in changes to the cellularity of the ipsilateral tibial bone marrow, which is innervated by the sciatic nerve (**Supplementary Fig. 3a**). Also, we found no difference in the numbers and frequencies of all examined immune cell populations including T cells, total B cells (**Supplementary Fig. 3b–d**), B cell subsets, granulocytes, NK cells, monocytes and DCs (data not shown). Taken together, CNS-induced (neurogenic) immune effects after spinal cord transection cannot result from direct denervation of lymphoid organs but rather must result from lesion-height-dependent (Th1 versus Th9) signaling involving spinal cord segments that innervate abdominal organs, including the adrenal glands.

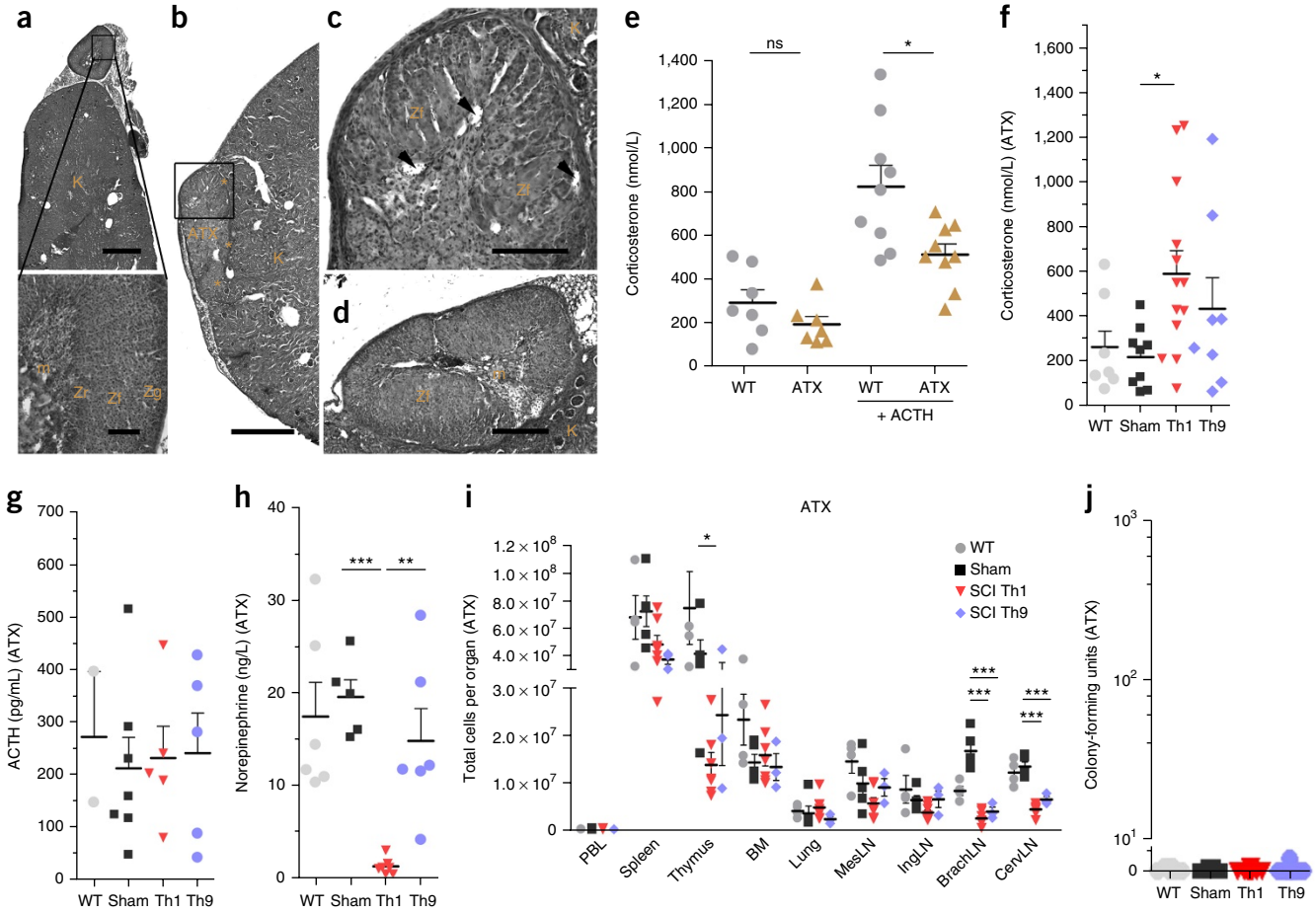

Figure 4 Interventional effects of autologous ATX after acute SCI. (**a**) The adrenal glands are located above the kidneys (K) and consist of a characteristic zonation (bottom panel shows enlargement of boxed area shown in top panel) including the CA-producing medulla (m) and the GC-producing cortex (Zr, zona reticularis; Zf, zona fasciculata; Zg, zona glomerulosa). Scale bars, 1 mm (top) and 100 µm (bottom). (**b**) Adrenotransplanted mice (in which both adrenal glands are transplanted under the ipsilateral kidney capsule) showed well-integrated transplants on hematoxylin and eosin (H&E)-stained histological sections (asterisks, kidney–adrenal border). Scale bar, 1 mm. (**c**) Higher-resolution image of boxed area in **b** demonstrates dense vascularization (arrowheads) and normal adrenocortical architecture. (**d**) In contrast, adrenal medulla (m) degenerated after transplantation, and small remnants were detectable only in a few sections. Scale bars in **c** and **d**, 200 µm. (**e**) ATX mice had normal serum corticosterone levels 6 weeks after transplantation, similar to wild-type controls (left; unpaired Student's *t* test, $P = 0.1790$, $t = 1.427$, $df = 12$; data are mean ± s.e.m., $n = 7$ animals per group), and they showed a physiological GC increase after ACTH administration (right; unpaired Student's *t* test, $^*P = 0.0115$, $t = 2.854$, $df = 16$; data are mean ± s.e.m., $n = 9$ animals per group). (**f**,**g**) In contrast to sham-operated mice, SCI in ATX mice resulted in only a small increase in serum corticosterone (**f**; one-way ANOVA, $P = 0.0479$, $F = 3.407$, $df = 29$, with Tukey's multiple comparison test, $^*P < 0.05$; data are mean ± s.e.m., $n = 8$ animals (Th9), 9 animals (sham), 13 animals (Th1)) and no suppression of ACTH concentration (**g**; one-way ANOVA, $P = 0.9450$, $F = 0.0568$, $df = 16$; data are mean ± s.e.m., $n = 5$ animals in each group (Th1, Th9), 7 animals (sham)). (**h**) Systemic NE levels were completely suppressed after Th1 (but not Th9) transection (one-way ANOVA, $P < 0.0001$, $F = 19.14$, $df = 17$, with Tukey's multiple comparison test, $^{**}P < 0.01$; $^{***}P < 0.001$; data are mean ± s.e.m., $n = 6$ animals (Th9), 5 animals (sham), 7 animals (Th1)). (**i**) After ATX, the differential effect after high vs. low thoracic level SCI (Th1 vs. Th9) on cell loss in spleen and LNs was largely abolished 3 d after SCI (one-way ANOVA, $P = 0.4569$, $F = 0.8366$, $df = 14$ (PBL); $P = 0.0523$, $F = 3.811$, $df = 14$ (spleen); $P = 0.0350$, $F = 4.492$, $df = 14$ (thymus); $P = 0.7620$, $F = 0.2780$, $df = 14$ (BM); $P = 0.4083$, $F = 0.1387$, $df = 14$ (lung), $P = 0.2358$, $F = 1.634$, $df = 14$ (mesLN); $P = 0.0754$, $F = 3.232$, $df = 14$ (ingLN); $P < 0.0001$, $F = 50.53$, $df = 14$ (brachLN); $P < 0.0001$, $F = 49.51$, $df = 14$ (cervLN), with Tukey's multiple comparison test, $^*P < 0.05$; $^{***}P < 0.001$; data are mean ± s.e.m., $n = 5$ animals (sham), 7 animals (Th1), 3 animals (Th9)). (**j**) In contrast to wild-type mice (cf. **Fig. 2d**) and ADX mice (**Fig. 3g**), none of the adrenotransplanted animals developed pneumonia after SCI (one-way ANOVA, $P = 0.9006$, $F = 0.1501$, $df = 29$; data are mean ± s.e.m.; ns, not significant; $n = 8$ animals (sham), 13 animals (Th1), 9 animals (Th9)).

Adrenalectomy prevents leukocyte depletion and lymphoid organ atrophy

Next, we tested whether dysfunctional innervation of the adrenal glands after SCI accounts for the observed changes. For this, we analyzed the effect of adrenalectomy (ADX) on lymphocyte behavior. Adrenal glands were bilaterally removed immediately before SCI surgery. ADX prevented the massive increase of serum corticosterone seen after injury (**Fig. 3a**), paralleled by the physiological response of ACTH secretion (**Fig. 3b**). ADX further resulted in approximately 60–70% reduction in systemic NE (**Fig. 3c**), suggesting that the remaining 30–40% derive from postganglionic sympathetic fibers extending not to the adrenal glands but to paraganglia throughout the abdominal cavity and lesser pelvis. Paralleling the GC depletion, ADX completely restored the size and cellularity of LNs, spleen and thymus after SCI (**Fig. 3d**,**e**), and the effect completely abolished the differences related to injury level (Th1 versus Th9; **Fig. 3f**). The normalization of cell numbers after ADX was relevant for all examined cell types including $CD19^+$ B cells, $CD4^+$ and $CD8^+$ T cells (**Supplementary Fig. 4a–c**),

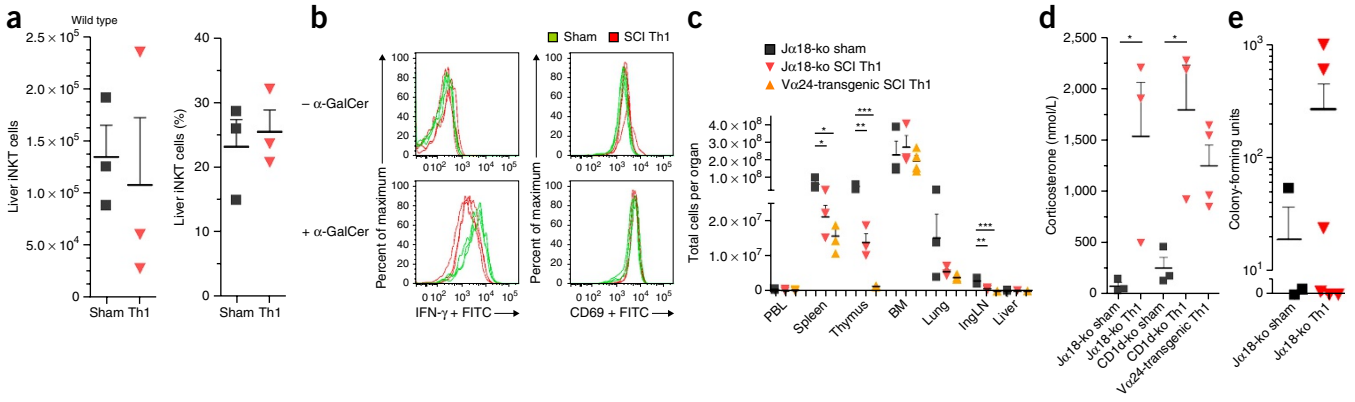

Figure 5 Liver iNKT cells do not interfere with infection susceptibility. (**a**) SCI did not affect the number or percentage of liver iNKT cells in wild-type mice (unpaired Student's *t* test, $P = 0.7234$, $t = 0.3798$, $df = 4$; data are mean ± s.e.m., $n = 3$ animals per group). (**b**) Top: SCI did not increase the expression of IFN-γ (left) or CD69 (right) in liver iNKT cells compared to sham mice. Bottom: as expected, α-galactosylceramide (α-GalCer) stimulation increased the expression of IFN-γ and CD69 in iNKT cells, but no further increases were seen after SCI. FITC, fluorescein isothiocyanate. (**c**) The absence of iNKT cells in the Jα18-knockout (ko) mouse or increased numbers of iNKT cells in the Vα24-transgenic mouse did not change the established pattern of immune cell depletion after SCI (one-way ANOVA, $P = 0.4100$, $F = 1.016$, $df = 9$ (PBL); $P = 0.0187$, $F = 7.417$, $df = 9$ (spleen); $P = 0.0006$, $F = 25.59$, $df = 9$ (thymus); $P = 0.6357$, $F = 0.4837$, $df = 9$ (BM); $P = 0.1215$, $F = 2.891$, $df = 9$ (lung); $P = 0.0003$, $F = 32.42$, $df = 9$ (ingLN); $P = 0.2635$, $F = 1.623$, $df = 9$, (liver), with Tukey's multiple comparison test, $^*P < 0.05$; $^{**}P < 0.01$; $^{***}P < 0.001$; data are mean ± s.e.m., $n = 3$ animals (Jα18-ko), 4 animals (Vα24-transgenic)). (**d**) Neuroendocrine changes were independent of the number of iNKT cells. Similarly to wild-type mice, Jα18-ko, CD1d-ko and Vα24-transgenic mice showed massive increases in serum corticosterone resulting from SCI (one-way ANOVA, $P = 0.0086$, $F = 5.925$, $df = 15$, with Tukey's multiple comparison test, $^*P < 0.05$; data are mean ± s.e.m., $n = 3$ animals per group (Jα18-ko, CD1d-ko), 4 animals (Vα24-transgenic)). (**e**) Lung infections were not pronounced in Jα18-ko mice with no iNKT cells (unpaired Student's *t* test, $P = 0.3592$ $t = 0.9811$, $df = 7$; data are mean ± s.e.m., $n = 3$ animals (sham), 6 animals (Th1)).

CD11c$^+$ DCs, and CD11b$^+$ monocytes (data not shown), as well as for LN morphology (**Fig. 3c**). No such reversal of cell populations was seen after removal of the spleen, another abdominal organ sympathetically innervated via the splanchnic nerve (**Supplementary Fig. 5**). Thus, the adrenal gland is the organ mediating cellular effects after SCI. Indeed, absence of the adrenal glands completely rescued the cellular phenotype, independent of the lesion height of SCI. However, despite normalization of leukocyte populations and lymphoid organ architecture, ADX did not prevent lung infections after SCI in mice (**Fig. 3g**).

We tested whether antagonism at the GC receptor could similarly prevent cell depletion and pneumonia. Mifepristone treatment indeed mitigated immune cell depletion, particularly in the thymus (**Fig. 3h**), but it could not prevent lung infections (**Fig. 3i**). Treatment with the β2-adrenergic antagonist propranolol and the β-adrenergic agonist isoproterenol led to 100% mortality in all SCI Th1 animals in two repeated cycles of experiments (data not shown).

Adrenotransplantation prevents spontaneous pneumonia

We next investigated the effect of maintaining basal corticosterone levels on leukocyte populations and susceptibility to infections, while preventing the SCI-induced GC excess by denervation of the adrenal glands. For this, glands were surgically removed and transplanted under the ipsilateral kidney capsule (adrenotransplantation, ATX; **Fig. 4a**,**b**), which disconnected them from spinal sympathetic innervation but allowed humoral responses via HPA-axis stimulation. Histological analyses demonstrated that ATX transplants were viable and vascularized (**Fig. 4b**,**c**). Adrenal medullary cells (which are modified postganglionic neurons) degenerated after disruption from their preganglionic autonomic nerve fibers in the transplant (**Fig. 4c**,**d**), leading to persistently reduced NE levels. However, after 6 weeks, mice had normal levels of serum corticosterone (**Fig. 4e**) and a physiological GC increase after ACTH administration (**Fig. 4e**). Following SCI, the increase in corticosterone was only mild and the previously shown difference between Th1- and Th9-injured animals was largely abolished for corticosterone levels and pituitary ACTH suppression (**Fig. 4f**,**g**). Systemic NE levels further declined after Th1 (but not Th9) transection (**Fig. 4h**), suggesting complete interruption of sympathetic outflow from the spinal cord. Also, the SCI-induced effects on organ size and cellularity were less pronounced in adrenotransplanted animals (**Fig. 4i**) compared to injured wild-type mice, including almost all immune cell populations (**Supplementary Fig. 6a–c**). Crucially, none of the adrenotransplanted mice developed spontaneous pneumonia (**Fig. 4j**). As ATX abolished cellular effects of lesion height and protected from pneumonia after SCI, we identified the sympathetic denervation of the adrenal gland and its maladaptive response as the decisive mechanism of SCI-IDS.

SCI-IDS is not mediated by liver invariant natural killer T cells

We next examined whether SCI-induced fluctuations of invariant natural killer T (iNKT) cells in the liver account for the enhanced susceptibility to acute lung infections after SCI, as suggested in experimental stroke[23]. iNKT cell numbers in the liver were relatively unchanged after SCI (**Fig. 5a**) and did not fluctuate in ADX and ATX animals (**Supplementary Fig. 7a**,**b**). In contrast to the stroke data, iNKT cells were not activated by injury, although they responded physiologically to stimulation with the iNKT-specific ligand α-galactosylceramide (**Fig. 5b**). The cell loss of immune organs after SCI was similar to that in wild-type mice and was not changed in iNKT transgenic or knockout mice (**Fig. 5c**). Finally, the injury-induced GC response was identical in two iNKT knockout strains, which have depleted iNKT cell numbers, and in one transgenic strain, which has increased iNKT cell numbers (**Fig. 5d**). The iNKT knockout mice did not develop more pronounced pneumonia (**Fig. 5e**), and animals of both genotypes were not more susceptible to death (data not shown). Thus, in contrast to cerebral ischemia models, iNKT cells did not mediate the susceptibility to pneumonia after experimental SCI.

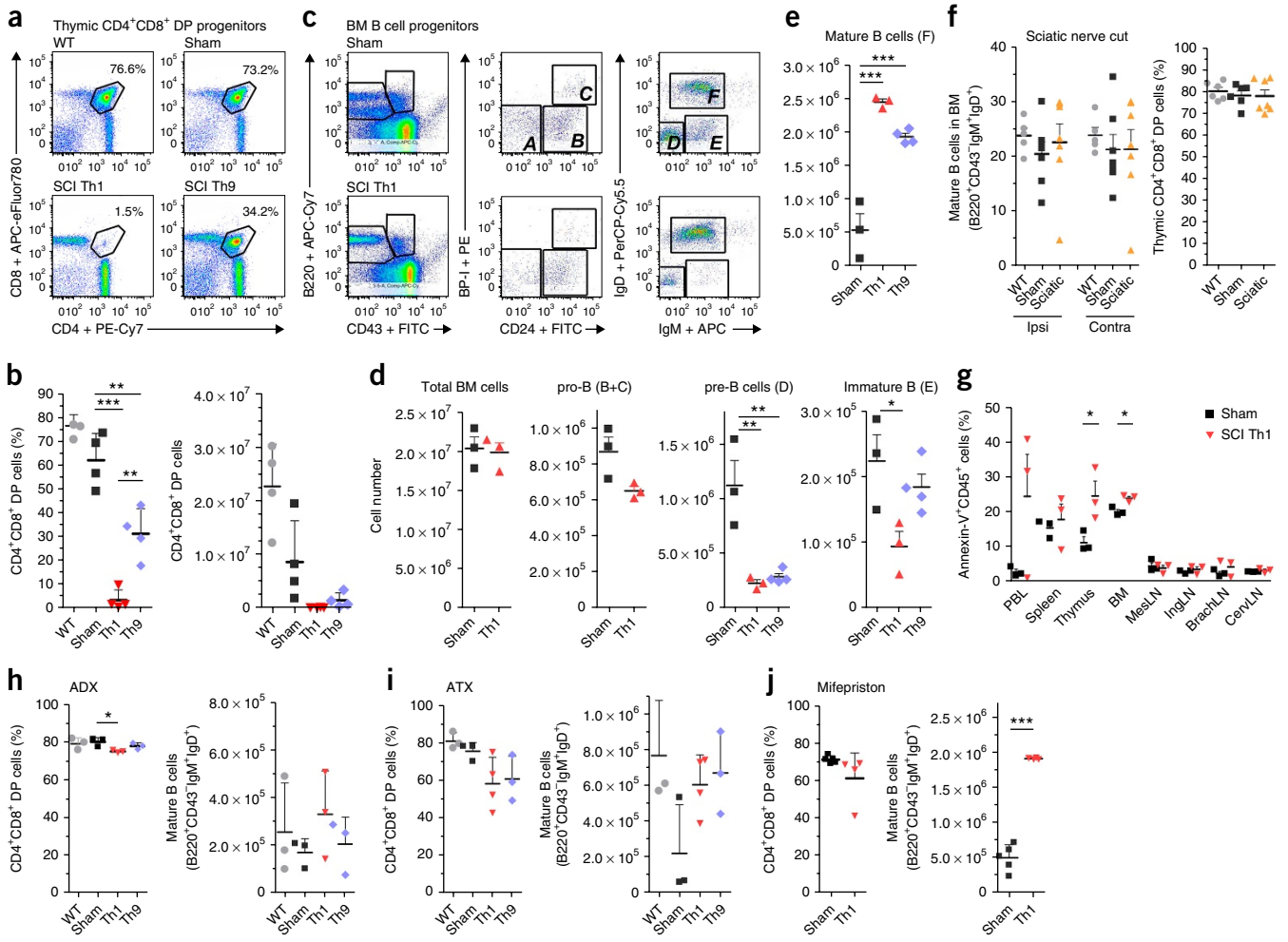

Figure 6 SCI-induced depletion of B and T cell progenitors. (**a**) Massive reduction in thymus cells 3 d after SCI mainly affected $CD4^+CD8^+$ double-positive (DP) progenitors. (**b**) Quantification of DP cells after SCI demonstrated their almost complete disappearance in a lesion-height-dependent manner (left, percentage; right, absolute DP cell number; one-way ANOVA, $P < 0.0001$, $F = 40.13$, $df = 11$, with Tukey's multiple comparison test, $^{**}P < 0.01$, $^{***}P = 0.001$; data are mean ± s.e.m., $n = 4$ animals per group). (**c**) Representative fluorescence-activated cell sorting (FACS) plots of BM 3 d after sham surgery or SCI. We determined B cell populations during development (populations A–F; Hardy nomenclature) based on CD43, B220, CD24, BP-I, IgM and IgD expression. (**d**) Quantification showed that early B cell populations in BM were profoundly reduced, ranging from pro-B cells (population B+C; unpaired Student's t test, $P = 0.0620$, $t = 2.570$, $df = 4$; data are mean ± s.e.m., $n = 3$ per group) to pre-B cells (population D; one-way ANOVA, $P = 0.0023$, $F = 16.38$, $df = 9$, with Tukey's multiple comparison test, $^{**}P < 0.01$; data are mean ± s.e.m., $n = 3$ animals in each group (Sham, Th1), 4 animals (Th9)) and immature B cells (population E; one-way ANOVA $P = 0.0386$, $F = 5.370$, $df = 9$, with Tukey's multiple comparison test, $^{*}P < 0.05$; data are mean ± s.e.m., $n = 3$ animals in each group (Sham, Th1), 4 animals (Th9)). (**e**) While progenitors and early B cells in BM were profoundly reduced, the number of mature IgM^+IgD^+ double-positive naive B cells (population F) markedly increased after high-level SCI (one-way ANOVA, $P < 0.0001$, $F = 51.35$, $df = 9$, with Tukey's multiple comparison test, $^{***}P < 0.001$; data are mean ± s.e.m., $n = 3$ animals in each group (Sham, Th1), 4 animals (Th9)). (**f**) Sciatic nerve (postganglionary) lesions had no effect on the composition of mature B cells in the ipsilateral (ipsi) and contralateral (contra) BM (left; unpaired Student's t test; $P = 0.6038$, $t = 0.5329$, $df = 12$ (ipsi); $P = 0.9894$, $t = 0.0135$, $df = 12$ (contra); data are mean ± s.e.m., $n = 7$ animals in each group (sham, sciatic)), and such lesions did not change the percentage of thymic $CD4^+CD8^+$ double-positive T cell precursors (right; unpaired Student's t test; $P = 0.9417$, $t = 0.0748$, $df = 11$; data are mean ± s.e.m., $n = 6$ animals (sham), 7 animals (sciatic)). (**g**) Apoptosis contributed to the loss of immune cell populations after SCI, as determined by the percentage of Annexin-V^+ cells (unpaired Student's t test, $P = 0.1450$ $t = 1.807$, $df = 4$, (PBL); $P = 0.6328$, $t = 0.5164$, $df = 4$, (spleen); $^{*}P = 0.0441$, $t = 2.900$, $df = 4$, (thymus); $^{*}P = 0.0113$, $t = 4.441$, $df = 4$, (BM); $P = 0.6728$, $t = 0.4549$, $df = 4$, (mesLN); $P = 0.4110$, $t = 0.9172$, $df = 4$, (ingLN); $P = 0.3102$, $t = 1.161$, $df = 4$, (brachLN); $P = 0.3700$, $t = 1.009$, $df = 4$, (cervLN); data are mean ± s.e.m., $n = 3$ animals per group). (**h**) The near-complete depletion of $CD4^+CD8^+$ double-positive precursor cells in the thymus after SCI is reversed with ADX (left; one-way ANOVA, $P = 0.0264$, $F = 7.076$, $df = 8$, with Tukey's multiple comparison test, $^{*}P < 0.05$; data are mean ± s.e.m., $n = 3$ animals per group), and the number of B cell progenitors in the BM was unchanged (right; one-way ANOVA, $P = 0.3427$, $F = 1.287$, $df = 8$; data are mean ± s.e.m., $n = 3$ animals per group). (**i**) Similarly, after ATX, we saw no significant differences in downregulation of thymic DP T cells (left; one-way ANOVA, $P = 0.1904$, $F = 2.122$, $df = 9$; data are mean ± s.e.m., $n = 3$ animals per group (WT, sham, Th9), 4 animals (Th1)) and recruited BM mature B cells (right) after Th1 versus Th9 SCI (one-way ANOVA, $P = 0.0774$, $F = 3.771$, $df = 9$; data are mean ± s.e.m., $n = 3$ animals in each group (sham, Th9), 4 animals (Th1)). (**j**) Mifepristone treatment reversed the SCI-induced loss of thymic progenitors (left; unpaired Student's t test, $P = 0.1385$, $t = 1.672$, $df = 7$; data are mean ± s.e.m., $n = 5$ animals (sham), 4 animals (Th1)) but did not normalize the BM enrichment of mature B cells (right; unpaired Student's t test, $^{***}P < 0.0001$, $t = 14.83$, $df = 7$; data are mean ± s.e.m., $n = 5$ animals (sham), 4 animals (Th1)).

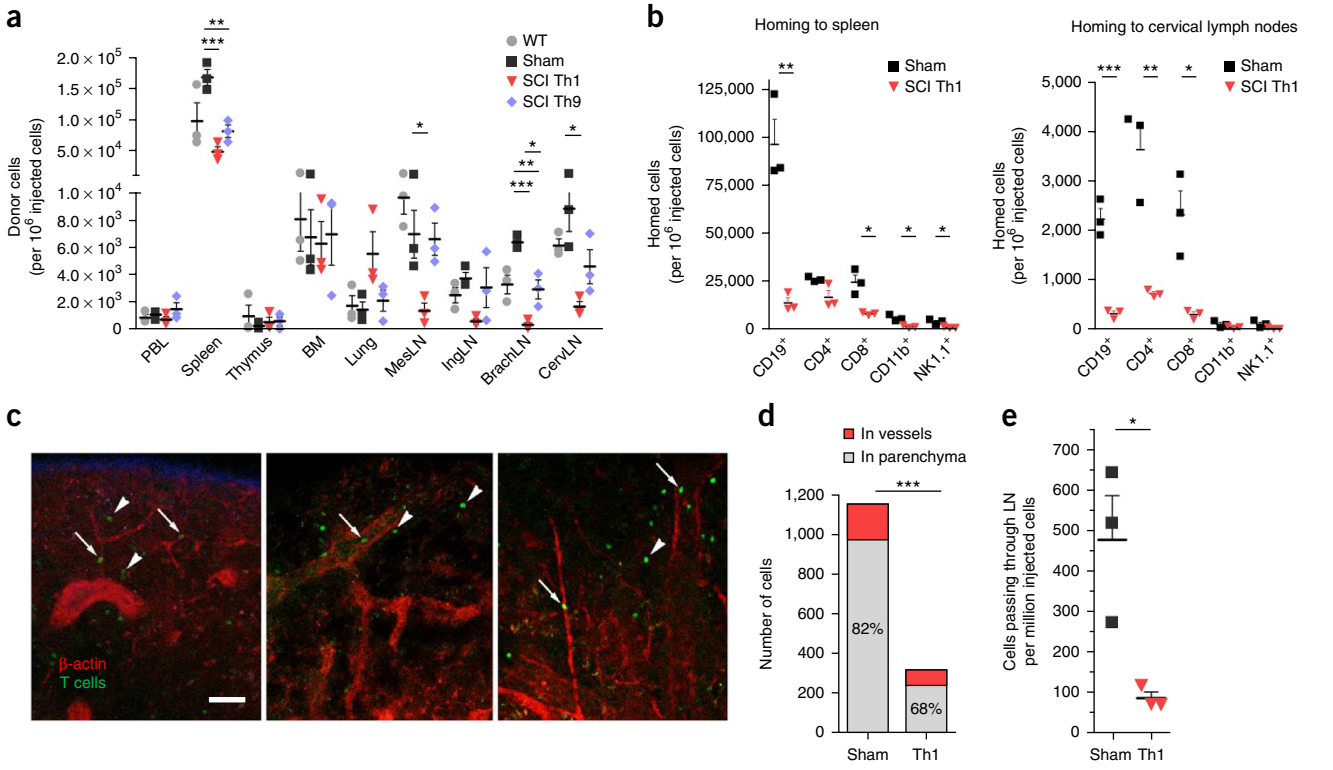

Figure 7 Impaired lymphocyte trafficking behavior after acute SCI. (**a**) Defective leukocyte homing to lymphoid organs after SCI is lesion-height-dependent (2-h homing of donor splenocytes, numbers normalized to 1 million injected cells) but also evident in non-denervated LN above the lesion (one-way ANOVA, $P = 0.3139$, $F = 1.414$, $df = 8$ (PBL); $P = 0.0005$, $F = 35.20$, $df = 8$ (spleen); $P = 0.6873$, $F = 0.3994$, $df = 8$ (thymus); $P = 0.9688$, $F = 0.0319$, $df = 8$ (BM); $P = 0.0783$, $F = 4.012$, $df = 8$ (lung); $P = 0.0350$, $F = 6.175$, $df = 8$ (mesLN); $P = 0.0986$, $F = 3.495$, $df = 8$ (ingLN); $P = 0.0002$, $F = 45.32$, $df = 8$ (brachLN); $P = 0.0166$, $F = 8.768$, $df = 8$ (cervLN), with Tukey's multiple comparison test, $^*P < 0.05$; $^{**}P < 0.01$; $^{***}P < 0.001$; data are mean ± s.e.m., $n = 3$ animals per group). (**b**) Homing of injected donor splenocytes was not equally impaired for all donor cell populations or target organs. Left: massive reduction of homing of all cell types to the spleen after SCI compared to sham with most pronounced homing deficit for CD19$^+$ B cells (unpaired Student's t test, $^{**}P = 0.0034$, $t = 6.206$, $df = 4$ (CD19$^+$); $P = 0.0625$, $t = 2.562$, $df = 4$ (CD4$^+$); $^*P = 0.0126$, $t = 4.307$, $df = 4$ (CD8$^+$); $^*P = 0.0148$, $t = 4.107$, $df = 4$ (CD11b$^+$); $^*P = 0.0278$, $t = 3.380$, $df = 4$ (NK1.1$^+$); data are mean ± s.e.m., $n = 3$ animals per group). Right: homing to cervical LNs was also largely reduced after SCI, but homing of donor cells was equally impaired for all cell populations (unpaired Student's t test, $^{***}P = 0.0009$, $t = 8.804$, $df = 4$ (CD19$^+$); $^{**}P = 0.0059$, $t = 5.348$, $df = 4$ (CD4$^+$); $^*P = 0.0139$, $t = 4.184$, $df = 4$ (CD8$^+$); $P = 0.2448$, $t = 1.362$, $df = 4$ (CD11b$^+$); $P = 0.1332$, $t = 1.880$, $df = 4$ (NK1.1$^+$); data are mean ± s.e.m., $n = 3$ animals per group). (**c**) Two hours after intravenous injection of labeled T cells (green), the majority of cells found in peripheral LNs were located outside blood vessels (arrowheads). Only few cells were marginated or flowed through venules (arrows). Left: note the LN architecture, with wide spaces between high endothelial venules (red, β-actin-RFP) and LN capsule (blue, second harmonic). Middle: after SCI, fewer total cells are found in peripheral LNs, with a higher percentage of cells still localized inside blood vessels. Right: deep vessels in a brachial LN after SCI. Scale bar, 100 µm. (**d**) Quantification showed markedly reduced total cell numbers in the LN but only a slight percentage reduction in the number of cells that transmigrate and are found in the parenchyma (68% (237 of 313) vs. 82% (974 of 1,153)) rather than in the vessels (χ^2 test, $^{***}P = 0.0003$; data are absolute frequencies, $n = 7$ brachLN from 3 animals per group). (**e**) *In vivo* imaging of ingLN showed reduced passage of injected lymphocytes through the node after SCI, suggesting impaired organ perfusion (unpaired Student's t test, $^*P = 0.0235$, $t = 3.563$, $df = 4$; data are mean ± s.e.m., $n = 3$ animals per group).

Lymphocyte progenitor cell loss, apoptosis and disturbed homing contribute to adrenal gland-mediated SCI-IDS

Next we investigated the mechanisms that led to the clinically detectable hallmark of SCI-IDS, injury-induced leukopenia, and whether they can be reversed by ADX and ATX. Given that most lymphocytes permanently circulate through lymphoid organs, the obvious cell depletion with organ shrinkage could result from (i) reduced availability of cells due to the loss of immune cell progenitors, (ii) increased apoptosis and clearance of lymphocytes or (iii) disturbed physiological cell migration or homing into bone marrow (BM) and LNs. Thus, we first investigated the effect of SCI on T and B cell progenitors. Indeed, thymic CD4$^+$CD8$^+$ double-positive progenitors of the T cell lineage were most affected, showing almost complete loss after Th1 SCI (**Fig. 6a**,**b**). Similarly, in the B cell lineage, B220$^+$CD43$^+$ progenitor B cell populations in the BM, ranging from pro-B to pre-B and immature B cells, decreased markedly (**Fig. 6c**,**d**). Notably, BM cellularity was not reduced despite SCI-induced depletion of B cell progenitors, because cell loss was fully compensated for by profound enrichment with mature B cells (**Fig. 6e**). These IgM$^+$IgD$^+$ double-positive B cells (population F), which normally mature in the spleen, preferentially re-entered the BM after SCI at a rate fivefold higher than in sham-operated animals. In line with the above-demonstrated GC-mediated rather than deafferentation-induced B cell changes, the cell populations were unchanged after sciatic nerve injury, i.e., interruption of the nerve fibers targeting tibial BM (**Fig. 6f**). Increased apoptosis contributed to leukopenia after SCI: in an independent set of experiments, mice were subjected to sham operations or Th1 SCI, resulting in the characteristic pattern of leukocyte depletion after 3 d.

Lymphoid organ cell suspensions analyzed by flow cytometry demonstrated an increased rate of AnnexinV$^+$ apoptotic cells in most organs, particularly in BM and thymus (**Fig. 6g**). The key role of the adrenal glands for progenitor cell loss was confirmed using ADX and ATX animals (**Fig. 6h**,**i**). In both conditions, the characteristic depletion of thymic DP progenitors and the SCI-associated enrichment of mature B cells in the BM were normalized, and the different effects of Th1 versus Th9 lesions were largely abolished (**Fig. 6h**,**i**). Mifepristone treatment reversed the SCI-induced loss of thymic progenitors but did not normalize the BM enrichment of mature B cells (**Fig. 6j**).

To determine the contribution of lymphocyte trafficking as an underlying mechanism for immune surveillance and host defense to immune dysfunction after SCI-IDS, we analyzed cell homing and redistribution through blood and lymphoid organs as described earlier[24]. Splenocytes of wild-type donor mice were injected into the tail veins of sham-operated and SCI mice. Injured animals (72 h after SCI) showed a severe 2-h homing deficit of donor cells to most organs, with exception of the BM (**Fig. 7a**), particularly for the spleen and lymph nodes (**Fig. 7b**). The homing deficit was much more pronounced after Th1 compared to Th9 lesions. However, homing was not equally impaired for all donor cell populations or target organs. For example, B cells were particularly excluded from homing to the spleen; the relative percentage of arriving B cells dropped from almost 60% to 30% in Th1-injured compared to sham-operated mice (**Supplementary Fig. 8a**). In cervical LNs, the homing deficit was similar for B and T cells (**Supplementary Fig. 8b**). The 2-h homing deficit was already detectable 1 d after SCI (**Supplementary Fig. 8c**). In addition to homing, redistribution of donor cells (15 h cell migration) was also severely disturbed after SCI (**Supplementary Fig. 8d**), collectively suggesting that SCI-induced trafficking deficits contribute to downstream mechanisms of SCI-IDS.

Reduced homing after SCI may also involve lymph node perfusion

We next investigated whether the SCI-related cell-trafficking impairment results from defective adhesion to secondary lymphoid organ endothelium. For this, *in vivo* imaging of the inguinal LN was performed. The rolling fraction of donor T cells injected via the contralateral femoral artery was not reduced in venules of SCI animals (**Supplementary Fig. 9a**). Accordingly, expression of peripheral lymph node addressin, the endothelial ligand mediating leukocyte rolling in lymphoid tissues, was clearly detectable or even increased in the LN, suggesting that LN shrinkage is not caused by dysfunctional leukocyte rolling (**Supplementary Fig. 9b**). Comparing the ratio of lymphocytes that left the vasculature with lymphocytes adhering to the LN vessel, we found that SCI resulted in slightly impaired transmigration across endothelium (68% versus 82%; **Fig. 7c**,**d**). We note, however, that the total numbers of injected T cells found in LN (both intravascular and extravascular) in this experiment were largely decreased after SCI despite normal rolling. Similarly, *in vivo* imaging of the inguinal LN showed a profound reduction in cells passing through the node, possibly reflecting diminished perfusion after SCI (**Fig. 7e**). Impaired LN perfusion would then implicate the contribution of a more global vascular mechanism related to cardiac output and sympathetic tone.

Homing to BM was different than to secondary lymphoid organs

As shown above, the overall number of BM cells was not reduced after SCI despite loss of B cell progenitor populations, and thus is in contrast with other lymphoid organs. We thus determined the contribution of cell trafficking to BM cellularity. Indeed, redistribution and migration were not impaired (**Supplementary Fig. 9c**), a finding that was paralleled by increased expression of homing molecules, such as C-X-C motif chemokine 12 (CXCL12), which attracts and activates leukocytes and of which real-time PCR showed a tenfold increase in BM mRNA expression (**Supplementary Fig. 9d**). SCI-induced preferential homing of mature B cells to BM was completely abolished when B cells had been pretreated *in vitro* with pertussis toxin, which inhibits the expression of leukocyte function-associated antigen 1 (LFA1) on B cells, thereby preventing LFA1-mediated transmigration into the organ (**Supplementary Fig. 9e**). Taking these data together, we observed a distinct homing behavior driving cells to BM rather than to secondary lymphoid organs (for example, spleen) after SCI.

DISCUSSION

We demonstrated that susceptibility to spontaneous pneumonia and severe lymphopenia after SCI resulted from a maladaptive sympathetic-neuroendocrine reflex involving the adrenal glands. Disrupting nerve fibers innervating the adrenal glands by high-level (Th1) but not low-level (Th9) thoracic spinal cord transection resulted in almost complete suppression of circulating norepinephrine levels and profound stimulation of systemic corticosterone levels. Congruent findings were seen in human patients with traumatic complete SCI. The data are in stark contrast to the classical concept of SCI-induced immunosuppression as being mainly mediated by stress-related noradrenergic overactivation and excess GC release via HPA-axis stimulation[3,25–28]. Instead, we report adrenal activation without HPA stimulation after SCI. Our data point to a two-step reflex mechanism (**Supplementary Fig. 10**) consisting of spinal-level-dependent disrupted innervation of the adrenal glands (neurogenic branch) followed by systemic effects of reduced CA and increased GC levels (circulatory branch). Based on our findings, we hypothesize that therapeutic normalization of the GC and CA imbalance in SCI patients could be a promising strategy to prevent detrimental infectious complications.

The sympathetic-neuroendocrine adrenal reflex

SCI-induced sympathetic deafferentation of the adrenal gland resulted in depletion of NE release from the adrenal medulla and disinhibition of GC release from the adrenal cortex (primary (i.e., adrenal) hypercortisolism), which in turn suppressed pituitary ACTH, constituting a maladaptive neuroendocrine reflex (or response). The sympathetic innervation of the GC-producing adrenal cortex has been known for a long time, and electrical stimulation of the splanchnic nerve can modulate steroid release[29,30]. Moreover, β-adrenergic stimulation inhibited DNA synthesis in the adrenocortical cells *in vivo*, suggesting that catecholaminergic nerves tonically inhibit adrenocortical cell function[31]. This mechanism was supported by findings in adrenotransplanted mice, in which the function of the adrenal glands was disconnected from spinal nerve innervation by transplantation under the kidney capsule. The cellular differences between high-level versus low-level SCI were largely abolished, as was the increase in GC levels. Critically, none of the adrenotransplanted mice developed pneumonia, suggesting that intact adrenal basal function protects from infection after SCI. The importance of restored physiological GC levels is supported by findings that different concentrations of GC can have opposite effects on the immune system[32]. In contrast, ADX alone or treatment with GC receptor antagonists did not prevent pneumonia after SCI, thus demonstrating that restoration of immune cell numbers is insufficient to reconstitute host defense. ATX likely provides the adequate 'titration' of GC levels for leukocyte function and surveillance, in contrast to ADX (very low GC levels) and Th1 SCI (very high levels).

The sympathetic-neuroendocrine adrenal reflex adds to the growing number of cross-regulation mechanisms between the nervous system and the immune system. These include the inflammatory reflex via the spleen, which can regulate inflammatory responses and can be triggered by vagus nerve and sympathetic stimulation[15,17,33]. SCI turned out to be an ideal experimental model for studying neurogenic reflex mechanisms, because of the relatively uniform anatomical structure along the rostrocaudal axis and the well-defined nervous connections emanating at different spinal levels. Low-level SCI (Th9) had some attenuated effect on adrenal function, likely because adrenal innervation receives fibers arising from spinal levels Th3 to L1[30]. The reflex described here involves the splanchnic nerve, which has recently been shown to be the efferent arm of a powerful anti-inflammatory reflex responding to intravenous lipopolysaccharide stimulation[15]. Thus, pathological stimulation of this reflex arc by high-level spinal lesions through lack of supraspinal sympathetic inhibition might further fuel functional SCI-IDS.

The sympathetic-neuroendocrine adrenal reflex causes systemic immunodeficiency

We identified several mechanisms by which SCI-induced adrenal dysfunction leads to immunosuppression. These included an early, massive loss of all major leukocyte populations in spleen, thymus and LNs; disturbed lymphocyte migration or homing to secondary lymphoid organs; increased apoptosis; and particular loss of B and T cell lineage progenitors. The adrenal glands are key organs for neurogenic immune effects after SCI, as ADX completely restored lymphoid tissue changes. Moreover, adrenal-derived CAs are required for leukocyte organ perfusion and for mobilizing leukocytes from the marginal pool (cells that roll along the endothelial layer)[34,35] and can increase peripheral lymphocyte populations by several hundred percent[36]. Thus, reduced NE levels likely facilitate margination and, in this way, further the reduction of leukocytes in peripheral blood. Unfortunately, we could not demonstrate the reversibility of immunosuppression with β-adrenergic drugs, as all animals died from treatment with propranolol and isoproterenol in doses previously demonstrated to be necessary for clinical effects[4,37,38]. Complete high-level cord transection is a rather severe SCI model, which likely causes an extent of sympathetic instability that is not compatible with further adrenergic manipulations.

It is noteworthy that local tissue levels of CAs can be regulated independently of the adrenal glands and can be increased in lymphoid organs despite depletion of systemic levels. Indeed, high-level SCI has been repeatedly shown to cause sustained increases in splenic NE with subsequent massive apoptosis of spleen lymphocytes[4,16,38,39]. One main difference between the SCI model and models of acute brain damage such as stroke is the sparing of the vagus nerve after thoracic SCI, which leaves the bidirectional parasympathetic connection between brainstem and abdominal organs intact. As different mechanisms after stroke versus SCI contribute to the immune deficiency, it is plausible that iNKT cells did not mediate susceptibility to infection after SCI in the present paper, while they did after experimental stroke[23].

A maladaptive adrenal reflex as a target for preventing prevalent infections

Taken together, acute SCI elicits a maladaptive sympathetic-neuroendocrine reflex, with the adrenal glands as key organs for immune effects after injury. The evidence provided here challenges several models. First, SCI-induced GC excess represents adrenal (primary) hypercortisolism rather than HPA-axis stimulation. Second, postganglionary deafferentation of lymphoid tissue seems to have no effect on lymphocyte trafficking, disrupted lymphoid organ morphology or susceptibility to infection. Third, strong NE reduction might lead to broader systemic cardiovascular effects contributing to an immunological SCI disease. We provide comprehensive evidence that, besides the loss of motor and sensory function, SCI also causes a graded immune paralysis, providing insights into how the CNS controls the immune system. This is of exceptional clinical importance, given the profoundly increased rate of infectious complications in SCI patients. Re-establishing near-baseline levels of GC after SCI prevented pneumonia, thus offering a potential therapeutic strategy for preventing infections in patients after CNS lesions.

METHODS

Methods, including statements of data availability and any associated accession codes and references, are available in the online version of the paper.

Note: Any Supplementary Information and Source Data files are available in the online version of the paper.

ACKNOWLEDGMENTS

We thank P. Popovich for critically reading the manuscript and insightful suggestions. We are grateful for the excellent technical help of D. Brandl, L. Mosch, C. Josties and I. Przesdzing. This work has been supported by grants from the German Academic Exchange Service (DAAD, D/10/43923) and German Research Foundation (DFG, PR 1274/2-1 to H.P.; STU 528/1-1, CRC-914 to S.S. and Cluster of Excellence NeuroCure to U.D.), by the Wings for Life Spinal Cord Research Foundation (WfL-DE-006/12), Else Kröner Fresenius Stiftung, German legal accident insurance (DGUV), the Era-Net-NEURON Program of the European Union, NIDILRR (#90SI5020), the Ohio State University Discovery Theme and the W.E. Hunt & C.M. Curtis Endowment to J.M.S. The National Spinal Cord Injury Database (NSCID) is funded by the National Institute on Disability, Independent Living, and Rehabilitation Research (NIDILRR, Grant number 90DP0083), US Department of Health and Human Services. This work was supported by the HMS Center for Immune Imaging and NIH grants AI112521 and AR068383 (to U.H.v.A.).

AUTHOR CONTRIBUTIONS

H.P., U.H.v.A. and J.M.S. designed the research study; H.P., A.Tedeschi, L.L., A. Thiriot, S.M.L., S.S., I.B.M., M.A.K., B.B., C.B., L.-C.G., T.L., A.N., F.B., M.S.V., M.J.D. and Y.C. conducted experiments and acquired data; all authors analyzed data; H.P., A. Thiriot, U.D., U.H.v.A. and J.M.S. wrote the manuscript; all authors contributed discussion to the manuscript.

COMPETING FINANCIAL INTERESTS

The authors declare no competing financial interests.

1. Steinman, L. Elaborate interactions between the immune and nervous systems. *Nat. Immunol.* **5**, 575–581 (2004).
2. Irwin, M.R. & Cole, S.W. Reciprocal regulation of the neural and innate immune systems. *Nat. Rev. Immunol.* **11**, 625–632 (2011).
3. Meisel, C., Schwab, J.M., Prass, K., Meisel, A. & Dirnagl, U. Central nervous system injury-induced immune deficiency syndrome. *Nat. Rev. Neurosci.* **6**, 775–786 (2005).
4. Lucin, K.M., Sanders, V.M. & Popovich, P.G. Stress hormones collaborate to induce lymphocyte apoptosis after high level spinal cord injury. *J. Neurochem.* **110**, 1409–1421 (2009).
5. Riegger, T. *et al*. Spinal cord injury-induced immune depression syndrome (SCI-IDS). *Eur. J. Neurosci.* **25**, 1743–1747 (2007).
6. Oropallo, M.A. *et al*. Chronic spinal cord injury impairs primary antibody responses but spares existing humoral immunity in mice. *J. Immunol.* **188**, 5257–5266 (2012).
7. Riegger, T. *et al*. Immune depression syndrome following human spinal cord injury (SCI): a pilot study. *Neuroscience* **158**, 1194–1199 (2009).
8. Furlan, J.C., Krassioukov, A.V. & Fehlings, M.G. Hematologic abnormalities within the first week after acute isolated traumatic cervical spinal cord injury: a case-control cohort study. *Spine* **31**, 2674–2683 (2006).
9. Brommer, B. *et al*. Spinal cord injury-induced immune deficiency syndrome enhances infection susceptibility dependent on lesion level. *Brain* **139**, 692–707 (2016).

10. DeVivo, M.J., Kartus, P.L., Stover, S.L., Rutt, R.D. & Fine, P.R. Cause of death for patients with spinal cord injuries. *Arch. Intern. Med.* **149**, 1761–1766 (1989).
11. Jackson, A.B. & Groomes, T.E. Incidence of respiratory complications following spinal cord injury. *Arch. Phys. Med. Rehabil.* **75**, 270–275 (1994).
12. Failli, V. *et al.* Functional neurological recovery after spinal cord injury is impaired in patients with infections. *Brain* **135**, 3238–3250 (2012).
13. Kopp, M.A. *et al.* Long-term functional outcome in patients with acquired infections after acute spinal cord injury. *Neurology* **88**, 892–900 (2017).
14. Borovikova, L.V. *et al.* Vagus nerve stimulation attenuates the systemic inflammatory response to endotoxin. *Nature* **405**, 458–462 (2000).
15. Martelli, D., Yao, S.T., McKinley, M.J. & McAllen, R.M. Reflex control of inflammation by sympathetic nerves, not the vagus. *J. Physiol. (Lond.)* **592**, 1677–1686 (2014).
16. Zhang, Y. *et al.* Autonomic dysreflexia causes chronic immune suppression after spinal cord injury. *J. Neurosci.* **33**, 12970–12981 (2013).
17. Ueno, M., Ueno-Nakamura, Y., Niehaus, J., Popovich, P.G. & Yoshida, Y. Silencing spinal interneurons inhibits immune suppressive autonomic reflexes caused by spinal cord injury. *Nat. Neurosci.* **19**, 784–787 (2016).
18. Meador, K.J. *et al.* Role of cerebral lateralization in control of immune processes in humans. *Ann. Neurol.* **55**, 840–844 (2004).
19. Walter, U. *et al.* Insular stroke is associated with acute sympathetic hyperactivation and immunodepression. *Eur. J. Neurol.* **20**, 153–159 (2013).
20. Williams, J.M. *et al.* Sympathetic innervation of murine thymus and spleen: evidence for a functional link between the nervous and immune systems. *Brain Res. Bull.* **6**, 83–94 (1981).
21. Felten, D.L., Ackerman, K.D., Wiegand, S.J. & Felten, S.Y. Noradrenergic sympathetic innervation of the spleen: I. Nerve fibers associate with lymphocytes and macrophages in specific compartments of the splenic white pulp. *J. Neurosci. Res.* **18**, 28–36, 118–121 (1987).
22. Previnaire, J.G., Soler, J.M., El Masri, W. & Denys, P. Assessment of the sympathetic level of lesion in patients with spinal cord injury. *Spinal Cord* **47**, 122–127 (2009).
23. Wong, C.H., Jenne, C.N., Lee, W.Y., Léger, C. & Kubes, P. Functional innervation of hepatic iNKT cells is immunosuppressive following stroke. *Science* **334**, 101–105 (2011).
24. Massberg, S. *et al.* Immunosurveillance by hematopoietic progenitor cells trafficking through blood, lymph, and peripheral tissues. *Cell* **131**, 994–1008 (2007).
25. Dembowsky, K., Czachurski, J., Amendt, K. & Seller, H. Tonic descending inhibition of the spinal somato-sympathetic reflex from the lower brain stem. *J. Auton. Nerv. Syst.* **2**, 157–182 (1980).
26. Tibbs, P.A., Young, B., McAllister, R.G. Jr. & Todd, E.P. Studies of experimental cervical spinal cord transection. Part III: Effects of acute cervical spinal cord transection on cerebral blood flow. *J. Neurosurg.* **50**, 633–638 (1979).
27. Rawe, S.E. & Perot, P.L. Jr. Pressor response resulting from experimental contusion injury to the spinal cord. *J. Neurosurg.* **50**, 58–63 (1979).
28. Young, W., DeCrescito, V., Tomasula, J.J. & Ho, V. The role of the sympathetic nervous system in pressor responses induced by spinal injury. *J. Neurosurg.* **52**, 473–481 (1980).
29. Edwards, A.V. & Jones, C.T. Autonomic control of adrenal function. *J. Anat.* **183**, 291–307 (1993).
30. Parker, T.L., Kesse, W.K., Mohamed, A.A. & Afework, M. The innervation of the mammalian adrenal gland. *J. Anat.* **183**, 265–276 (1993).
31. Holzwarth, M.A., Cunningham, L.A. & Kleitman, N. The role of adrenal nerves in the regulation of adrenocortical functions. *Ann. NY Acad. Sci.* **512**, 449–464 (1987).
32. Dhabhar, F.S. & McEwen, B.S. Enhancing versus suppressive effects of stress hormones on skin immune function. *Proc. Natl. Acad. Sci. USA* **96**, 1059–1064 (1999).
33. Andersson, U. & Tracey, K.J. Neural reflexes in inflammation and immunity. *J. Exp. Med.* **209**, 1057–1068 (2012).
34. Dimitrov, S. *et al.* Cortisol and epinephrine control opposing circadian rhythms in T cell subsets. *Blood* **113**, 5134–5143 (2009).
35. Scheiermann, C. *et al.* Adrenergic nerves govern circadian leukocyte recruitment to tissues. *Immunity* **37**, 290–301 (2012).
36. Schedlowski, M. *et al.* Catecholamines modulate human NK cell circulation and function via spleen-independent beta 2-adrenergic mechanisms. *J. Immunol.* **156**, 93–99 (1996).
37. Prass, K. *et al.* Stroke-induced immunodeficiency promotes spontaneous bacterial infections and is mediated by sympathetic activation reversal by poststroke T helper cell type 1-like immunostimulation. *J. Exp. Med.* **198**, 725–736 (2003).
38. Lucin, K.M., Sanders, V.M., Jones, T.B., Malarkey, W.B. & Popovich, P.G. Impaired antibody synthesis after spinal cord injury is level dependent and is due to sympathetic nervous system dysregulation. *Exp. Neurol.* **207**, 75–84 (2007).
39. Rouleau, P., Ung, R.V., Lapointe, N.P. & Guertin, P.A. Hormonal and immunological changes in mice after spinal cord injury. *J. Neurotrauma* **24**, 367–378 (2007).

ONLINE METHODS

Animals. Female C57BL/6 wild-type mice, male β-actin-RFP mice (purchased from Charles River) and male iNKT Vα24-transgenic and knockout mice ($J\alpha18^{-/-}$, $CD1d^{-/-}$; kindly provided by Mark A Exley, Brigham and Women's Hospital, Boston) were housed in the animal facilities of the New Research Building, Harvard Medical School, or Children's Hospital Boston (Boston, USA) and were used at 6–10 weeks of age.

Spinal cord transection. Animals were anesthetized with a mixture of ketamine (80 mg/kg) and xylazine (10 mg/kg). Skin was shaved and disinfected with Betadine, followed by alcohol, three times. To determine the extent to which neurogenic effect of lesion level depended upon sympathetic nervous system deafferentation of the adrenal glands, we completely transected spinal cords at Th1 or Th9. After a dorsal incision along the vertebral column, overlying muscle was dissected. A dorsal Th1 or Th9 laminectomy was performed to expose the spinal cord and completely transect the spinal cord using a microknife (bleeding was controlled by surgical sponges). After assessing the completeness of the cut (i.e., presence of a gap between rostral and caudal end), dorsal muscle layers were sutured (6-0 PDS II suture) and the skin closed using sterile wound clips (7 mm). Animals with inconsistent lesion severity (tissue bridges) were removed from the study. This assured a complete interruption of supraspinal efferents to sympathetic preganglionic neurons (intermediolateral columns and funiculus lateralis), thereby disconnecting autonomic afferents to the adrenal gland[9]. Mice were provided with heating pads in their cages to prevent drops in body temperature because of their paralyzed hind limbs. Animals were checked twice per day for 3 d, and saline was administered and the bladder expressed at each check. Data collection and analysis were not performed blind to the conditions of the experiments.

Adrenalectomy. Under ketamine/xylazine anesthesia, skin was cleaned and dorsal skin was incised along the midline overlaying vertebrae T6–T8. Abdominal muscles were incised longitudinally on both sides. Left and right kidneys were slightly retracted with fine forceps to expose each adrenal gland. The entire adrenal gland was removed with a second pair of sterile, fine, curved forceps. Dorsal muscle layers were sutured and the skin closed using sterile wound clips (7 mm). Adrenalectomies were performed during the same anesthesia as used for experimental SCI. Animals were allowed to recover on a heating pad (37 °C) before we returned them to their cages.

Adrenotransplantation. The entire adrenal glands on both sides were removed as described under the "Adrenalectomy" section above. The kidney capsule was incised with fine forceps to expose the subcapsular space. Each adrenal gland was placed under the ipsilateral kidney capsule. The wound was sutured and closed as above. Mice were used for further experiments after 6 weeks.

Sciatic nerve injury. Under ketamine/xylazine anesthesia, skin was cleaned and a dorsal skin incision performed ~1 cm from midline. Muscles were carefully extended and the sciatic nerve retracted with a fine forceps, and a 1-mm segment of the nerve was excised. The skin was closed using sterile sutures.

Single cell suspension of immune organs. Mice were killed by CO_2 overdoses, and peripheral blood leukocytes (PBL, 500 µL) were obtained by cardiac puncture. Lymphocyte counts in PBL were determined with a Drew Hemavet (CDC Technologies, Oxford, CT). Single-cell suspensions were generated from spleens, peripheral LNs (2 brachial, 2 cervical, 2 inguinal), thymus, mesenteric LNs, Peyer's patches, BM, liver and lungs by forcing the tissues through a fine wire mesh. Bone marrow (BM) cells were harvested from one limb (corresponding to 10% of total BM). Cells were washed and resuspended in 1 mL PBS containing 1% FCS. Cell counts were performed in duplicates.

Homing assays. Splenocytes were isolated as single-cell suspensions from wild-type C57Bl/6 mice and fluorescently labeled with carboxyfluorescein diacetate succinimidyl ester (CFSE; Molecular Probes). Cells were injected intravenously (5 million per mouse) into sham-operated or SCI mice at 1 d (**Supplementary Fig. 8a**) or 3 d after SCI (**Fig. 7a**,**b**). After 2 h or 15 h, mice were killed for analysis and organs prepared for single-cell suspension as described above.

Analysis of spontaneous pneumonia. Lungs were removed under sterile conditions after thoracotomy and homogenized. Single-cell suspensions were resuspended in 1 mL PBS. For determination of CFU, 100 µL of the resuspended solutions were serially diluted, plated onto blood agar plates (Merck) and incubated at 37 °C for 24 h, after which bacterial colonies were counted. The homogenization of lung tissue and subsequent assessment of colony-forming units on blood agar plates with serially diluted samples is a standard procedure in diagnosing experimental pneumonia and enabled us to quantify the bacterial load as a surrogate for infection susceptibility[9]. Experimental pneumonia demonstrated all hallmarks of human pneumonia, including massive infiltration of immune cells and edema formation[9].

Drug administration. Drugs (all from Sigma-Aldrich) were injected i.p. (propranolol, mifepristone) or s.c. (isoproterenol), and the respective diluents were given to control animals in parallel. The β2-adrenergic receptor antagonist propranolol (30 mg/kg body weight, dissolved in 0.9% sodium chloride) was administered immediately before and 4 h and 8 h after SCI. The glucocorticoid receptor antagonist mifepristone (also called RU486; 30 mg/kg body weight, dissolved in ethanol:sesame oil (1:10)) was injected immediately before SCI and at 1 d and 2 d after injury. The β-adrenergic agonist isoproterenol (15 mg/kg body weight, dissolved in PBS) was administered twice per day.

Pertussis toxin (Ptx) pretreatment. Splenocytes were prepared from wild-type and CD45.1 mice and stained with CFSE as above. $CD45.1^+$ splenocytes were treated with Ptx (final concentration 200 ng/mL) for 2 h at 37 °C and washed with RPMI containing 2% FCS. We injected 4 million wild-type and Ptx-treated splenocytes (in 200 µL solution) into the tail veins of Bl/6 mice 2 d after Th1 SCI or sham surgery. After 24 h, organs were prepared and cell homing determined.

Intravital microscopy of inguinal lymph nodes (LNs). IVM of mouse inguinal LN was performed as described[40]. T cells from spleen and LN were purified (>90%) using the Pan T cell Isolation Kit II for mice (Miltenyi). Purified T cells were labeled with calcein AM (Molecular Probes) and small boluses of cells were injected intra-arterially (femoral artery). Lymphocyte–HEV interactions were recorded and analyzed offline as described[40]. The rolling fraction is defined as the percentage of fluorescent cells interacting with an HEV in the total number of cells passing through the vessel.

Transmigration. T cells from spleen and LN were purified (>90%), labeled with 5 µM 5-(and-6)-carboxyfluorescein diacetate succinimidyl ester (CMFDA, SE; Molecular Probes) and injected intravenously into β-actin-RFP mice (16 million per mouse). After 2 h mice were killed for analysis and the organs removed. Inguinal, brachial and cervical LN were prepared for two-photon microscopy. Three-dimensional analysis of cell localization relative to RFP^+ HEV was performed using Volocity software (Improvision, Lexington, MA).

Quantitative PCR. Total BM was isolated from femurs and tibias and mRNA prepared using RNeasy Mini kit according to the manufacturer's instructions (Qiagen). qPCR for CXCL12 (C-X-C motif chemokine 12) was performed with FastStart SYBR Master (Roche) using the primers CCAAACTGTGCCCTTCAGAT (forward) and ATTTCGGGTCAATGCACACT (reverse).

FACS analysis. For flow cytometric analysis the following fluorescently labeled monoclonal antibodies against the following antigens were obtained from BD Biosciences (Franklin Lakes, NJ): PE-labeled anti-CD19 (clone 1D3, catalog number #557399, 1:200 dilution), PE anti-BP-1 (BP1, #553735, 1:100), PE-Cy7 anti-CD11c (HL3, #558079, 1:100), APC anti-CD11b (M1/70, #553312, 1:100), APC anti-IgM (II/41, #550676, 1:100), FITC anti-IFNγ (XMG1.2, #554411, 1:100), FITC anti-CD69 (H1.2F3, #557392, 1:100), FITC anti-CD24 (M1/69, #553261, 1:100), APC-Cy7 anti-B220 (RA3-6B2, #552094, 1:100), biotinylated anti-CD43 (S7, #553269, 1:200) and PerCP-Cy5.5 anti-NK1.1 (PK136, #551114, 1:200). The following were obtained from BioLegend (San Diego, CA): PE-Cy7 anti-CD4 (GK1.5, #100422, 1:100) and PerCP-Cy5.5 anti-IgD (11-26c.2a, #405709, 1:100); and the following were obtained from eBioscience/Thermo Fisher (Waltham, MA): APC-eFluor780 anti-CD8 (53-6.7, #47-0081, 1:100), PerCP-eFluor710 anti-PDCA1 (927, #46-3172, 1:100) and PE-Cy7 anti-CD45 (30-F11, #25-0451,

doi:10.1038/nn.4643

1:100). In blood and spleen samples, RBCs were lysed with BD Lysis Solution (Becton Dickinson) before analysis. The degree of apoptotic cell death was quantified using fluorescein-labeled Annexin-V (Qbiogene). Cell phenotyping and identification of apoptotic cells was performed by six-color flow cytometry on a FACSCanto using CELLQuest software (BD Biosciences).

Immunohistochemistry. Frozen sections were prepared and subjected to a series of blocking with normal goat serum and washing procedures with PBS. Sections were incubated with anti-B220 to detect B-cell follicles (BD Biosciences, clone RA3-6B2, catalog #553084, 1:200 dilution), CD31 (BD, clone MEC13.3, #553370) or biotinylated anti-PNAd (peripheral lymph node addressin; Novus Biologicals, Littleton, CO, clone MECA-79, catalog #NB100-77674, 1:300) at 4 °C overnight, followed by incubation with the FITC-conjugated secondary antibody (Thermo Fisher) or with Alexa Fluor 488-conjugated streptavidin (Thermo Fisher, #S11223) for 60 min at 18–22 °C. The FITC-labeled cells were observed with a confocal laser scanning microscopy (Bio-Rad). Sections were cut at 10 μm.

ELISA for murine corticosterone, ACTH and norepinephrine. Corticosterone was analyzed by competitive-enzyme immunoassay (RE52211, IBL, Hamburg, Germany) from serum, ACTH was analyzed by sandwich ELISA (SG51041, IBL) from plasma and norepinephrine was analyzed from mouse plasma using an ELISA kit combining affinity extraction on a boronate-matrix with sandwich immunoassay (RE59261, IBL), according to the manufacturer's instructions. Determination was based on a four-parameter logistic (corticosterone, norepinephrine) or linear (ACTH) regression of standard analyte concentrations using GraphPad PRISM. Parallel processing of reference specimen served as quality control.

Cortisol measurements in SCI patients. Twenty patients with acute complete SCI (ASIA impairment scale (AIS) A) and 19 patients with acute vertebral fractures without SCI enrolled in a monocenter study associated with the "SCIentinel trial" after meeting eligibility criteria according to the published study protocol[41]. All patients underwent spinal surgery. Patients treated with systemic corticosteroids or with incomplete SCI were excluded. There were no differences between SCI patients and vertebral fracture patients regarding age (median, 47 years; interquartile range, 25.25–67.5 vs. median, 58; IQR, 46–60; $P = 0.221$), sex ($n = 17$, 85% male vs. $n = 15$, 79% male; $P = 0.695$), multiple injuries ($n = 4$, 20% vs. $n = 1$, 5%; $P = 0.342$) or time of day when blood was collected (median, 12.5 h; interquartile range, 8.25–15.0 h vs. median, 12.75 h; IQE, 9.66–16.0 h; $P = 0.674$). The neurological SCI level was above C6 in 13 patients (10 were injured at C4, two at C5 and one at C6) and below Th8 in 7 patients (two at Th8, one at Th9, two at Th12 and two at L2). Blood samples and data on CA treatment were collected within 96 h after SCI. Serum/plasma samples were centrifuged within 0.5–6 h after blood collection and frozen immediately for storage at −80 °C. ELISA measures were applied using pseudonymized patient samples according to the manufacturer (IBL International, Hamburg, Germany). The laboratory investigator was blinded to the clinical characteristics of the patients.

Neuroepidemiology of pneumonia after human SCI. Epidemiologic datasets indicating the occurrence of pneumonia after SCI were obtained from the National Spinal Cord Injury Database (NSCID) at the National Spinal Cord Injury Statistical Center, Birmingham, AL, USA. Data were collected prospectively in 25 specialized SCI care centers (Model Spinal Cord Injury Systems) from patients whose injuries were of acute traumatic etiology as previously described[12]. Eligibility criteria were complete neurological examination data according to the *International Standards for Neurological Classification of Spinal Cord Injury* (ISNCSCI) at hospital admission within 24 h after SCI and available documentation of pneumonia until discharge from inpatient rehabilitation. Patients with motor-complete traumatic SCI ASIA impairment scale (AIS) A or B and the single neurological level Th1–Th3 or Th9–Th12 were selected for analysis. We included 643 acute traumatic SCI patient datasets. Patients injured at neurological level Th1–Th3 ($n = 182$) and Th9–Th12 ($n = 461$) at admission were compared for the occurrence of radiologically confirmed pneumonia from admission until discharge from inpatient care. The groups (Th1–Th3 versus Th9–Th12 were not significantly different in terms of age (median, 30 years; interquartile range, 21–41 years vs. median, 29; IQR, 21–39; $P = 0.071$), sex ($n = 155$, 85% male vs. $n = 384$, 83% male; $P = 0.562$) and complete SCI ($n = 156$, 86% AIS A vs. $n = 370$, 80%; $P = 0.106$).

Statistical analysis. The distribution of continuous variables was described as mean ± standard error of mean (s.e.m.) unless otherwise noted. Data distribution was assumed to be normal, but this was not formally tested. Categorical variables were reported as frequencies and percentages. No statistical methods were used to predetermine sample sizes, but our sample sizes are similar to those reported in previous publications[9,23,37,42]. Continuous variables were analyzed using the Students *t* test. For comparison of multiple groups, one-way ANOVA followed by Tukey's *post hoc* test was applied. Categorical data were compared using the χ^2 test or Fisher's exact test where appropriate (in Prism version 5.0, GraphPad Inc.). For adjustment of clinical data, a linear regression model with cortisol levels as dependent variable and SCI as an independent variable was calculated and subsequently adjusted for age, gender and multiple injuries. The dependent variable was used after logarithmic transformation to achieve a normal distribution of the residuals (SPSS version 19.0, IBM Inc.). When provided, wild-type animals served as a descriptive reference group and were not included into the statistical testing, except for evaluation of the ADX and ATX models. All tests were two-sided and differences were considered statistically significant when $P < 0.05$.

Study approval. All mice were used according to current guidelines, and all experiments approved by the Harvard Medical School and the Children's Hospital (Boston, USA) and by the Berlin LaGeSo (Berlin, Germany) Standing Committee on Animals. Written informed consent was received from participants or their representatives before inclusion in the study, and analyses were approved by the Charité University Hospital Institutional Review Board or the institutional review boards of the centers contributing to the National Spinal Cord Injury Database. All clinical investigations were conducted according to *Declaration of Helsinki* principles. A **Life Sciences Reporting Summary** is available.

Data availability. The data that support the findings of this study are available from the corresponding author upon reasonable request.

40. von Andrian, U.H. Intravital microscopy of the peripheral lymph node microcirculation in mice. *Microcirculation* **3**, 287–300 (1996).
41. Kopp, M.A. *et al*. The SCIentinel study--prospective multicenter study to define the spinal cord injury-induced immune depression syndrome (SCI-IDS)--study protocol and interim feasibility data. *BMC Neurol*. **13**, 168 (2013).
42. Fatima, G., Sharma, V.P. & Verma, N.S. Circadian variations in melatonin and cortisol in patients with cervical spinal cord injury. *Spinal Cord* **54**, 364–367 (2016).

nature research

Corresponding author(s): Ulrich H. von Andrian

☐ Initial submission ☐ Revised version ☒ Final submission

Life Sciences Reporting Summary

Nature Research wishes to improve the reproducibility of the work that we publish. This form is intended for publication with all accepted life science papers and provides structure for consistency and transparency in reporting. Every life science submission will use this form; some list items might not apply to an individual manuscript, but all fields must be completed for clarity.

For further information on the points included in this form, see Reporting Life Sciences Research. For further information on Nature Research policies, including our data availability policy, see Authors & Referees and the Editorial Policy Checklist.

Experimental design

Sample size

Describe how sample size was determined.	No statistical methods were used to pre-determine sample sizes but our sample sizes are similar to those reported in previous publications [Brommer, B., et al. Brain 139, 692-707 (2016); Wong, C.H., et al. Science 334, 101-105 (2011); Prass, K., et al. J Exp Med 198, 725-736 (2003); Fatima, G., et al. Spinal Cord 54, 364-367 (2016)].

Data exclusions

Describe any data exclusions.	No data were excluded from the analyses. After surgical spinal cord injury, animals with inconsistent lesion severity (tissue bridges) were removed from the study.

Replication

Describe whether the experimental findings were reliably reproduced.	All attempts at replication were successful. Data points in the animal experiments after SCI are independent and do not represent technical replicates.

Randomization

Describe how samples/organisms/participants were allocated into experimental groups.	The experimental procedure of spinal cord injury could not be randomized as the lesion patterns make the animal group obvious to the examiner (high-level versus low-level SCI).

Blinding

Describe whether the investigators were blinded to group allocation during data collection and/or analysis.	After organ sampling from SCI animals, single-cell suspension were blinded to subsequent FACS analysis. Measurement of catecholamins and steroids (ELISA) was performed blinded to the experimental groups (SCI animals and human patients).

Note: all studies involving animals and/or human research participants must disclose whether blinding and randomization were used.

Nature Neuroscience: doi:10.1038/nn.4643

6. Statistical parameters

For all figures and tables that use statistical methods, confirm that the following items are present in relevant figure legends (or in the Methods section if additional space is needed).

n/a	Confirmed
☐	☒ The exact sample size (*n*) for each experimental group/condition, given as a discrete number and unit of measurement (animals, litters, cultures, etc.)
☐	☒ A description of how samples were collected, noting whether measurements were taken from distinct samples or whether the same sample was measured repeatedly
☐	☒ A statement indicating how many times each experiment was replicated
☐	☒ The statistical test(s) used and whether they are one- or two-sided (note: only common tests should be described solely by name; more complex techniques should be described in the Methods section)
☐	☒ A description of any assumptions or corrections, such as an adjustment for multiple comparisons
☐	☒ The test results (e.g. *P* values) given as exact values whenever possible and with confidence intervals noted
☐	☒ A clear description of statistics including central tendency (e.g. median, mean) and variation (e.g. standard deviation, interquartile range)
☐	☒ Clearly defined error bars

See the web collection on statistics for biologists for further resources and guidance.

Software

Policy information about availability of computer code

7. Software

Describe the software used to analyze the data in this study.	Routine commercial software was used: Prism Version 5.0, GraphPad Inc.; SPSS, Version 19.0, IBM Inc.

For manuscripts utilizing custom algorithms or software that are central to the paper but not yet described in the published literature, software must be made available to editors and reviewers upon request. We strongly encourage code deposition in a community repository (e.g. GitHub). *Nature Methods* guidance for providing algorithms and software for publication provides further information on this topic.

Materials and reagents

Policy information about availability of materials

8. Materials availability

Indicate whether there are restrictions on availability of unique materials or if these materials are only available for distribution by a for-profit company.	No unique materials were used.

Nature Neuroscience: doi:10.1038/nn.4643

9. Antibodies

Describe the antibodies used and how they were validated for use in the system under study (i.e. assay and species).

BD Biosciences (Franklin Lakes, NJ):
PE-labeled anti-CD19+ (clone 1D3, catalogue number #557399, 1:200 dilution),
PE anti-BP-1 (BP1, #553735, 1:100),
PE-Cy7 anti-CD11c+ (HL3, #558079, 1:100),
APC anti-CD11b+ (M1/70, #553312, 1:100),
APC anti-IgM (II/41, #550676, 1:100),
FITC anti-IFNγ (XMG1.2, #554411, 1:100),
FITC anti-CD69 (H1.2F3, #557392, 1:100),
FITC anti-CD24 (M1/69, #553261, 1:100),
APC-Cy7 anti-B220 (RA3-6B2, #552094, 1:100),
biotinylated anti-CD43 (S7, #553269, 1:200),
PerCP-Cy5.5 anti-NK1.1+ (PK136, #551114, 1:200);

BioLegend (San Diego, CA):
PE-Cy7 anti-CD4+ (GK1.5, #100422, 1:100),
PerCP-Cy5.5 anti-IgD (11-26c.2a, #405709, 1:100);

eBioscience/Thermo Fisher (Waltham, MA):
APC-eFluor780 anti-CD8+ (53-6.7, #47-0081, 1:100),
PerCP-eFluor710 anti-PDCA1+ (927, #46-3172, 1:100),
PE-Cy7 anti-CD45 (30-F11, #25-0451, 1:100).

The catalogue number of each antibody is linked to a data sheet on the supplier's homepage containing information on species validation and references.

10. Eukaryotic cell lines

a. State the source of each eukaryotic cell line used.

No eukaryotic cell lines were used.

b. Describe the method of cell line authentication used.

No eukaryotic cell lines were used.

c. Report whether the cell lines were tested for mycoplasma contamination.

No eukaryotic cell lines were used.

d. If any of the cell lines used are listed in the database of commonly misidentified cell lines maintained by ICLAC, provide a scientific rationale for their use.

No commonly misidentified cell lines were used.

Animals and human research participants

Policy information about studies involving animals; when reporting animal research, follow the ARRIVE guidelines

11. Description of research animals

Provide details on animals and/or animal-derived materials used in the study.

The following mice were used:
female C57BL/6 wild-type mice (Charles Rivers),
male β-actin-RFP mice (Charles River),
male iNKT Vα24-transgenic and knockout mice (Jα18-/-, CD1d-/-) (kindly provided by Mark A Exley, Boston).
Age: 6–10 weeks.

Policy information about studies involving human research participants

12. Description of human research participants

Describe the covariate-relevant population characteristics of the human research participants.

20 patients with acute complete SCI (ASIA impairment scale [AIS] A) and 19 patients with an acute vertebral fracture without SCI enrolled in a monocenter study associated to the 'SCIentinel trial' after meeting the inclusion criteria according to the published study protocol were included (Kopp MA et al. 2013, BMC Neurol 13, 168). All patients underwent spinal surgery. Patients treated with systemic corticosteroids or with incomplete SCI were excluded. There were no differences between SCI patients and vertebral fracture patients regarding age (mean 47 years [range 25.25-67.5] vs. 58 [46-60], p=0.41), sex (85% male vs. 79%, p=0.7) and multiple injuries (20% vs. 5%, p=0.34). Blood samples and data on medical treatment were collected within 96 hours after SCI.

Nature Neuroscience: doi:10.1038/nn.4643